



1 **Long-term variability of Norway lobster (*Nephrops norvegicus*) landings in relation to**  
2 **a changing climate in the Northwestern Mediterranean Sea.**

3 Mireia G. Mingote<sup>1,2,3</sup>, Frédéric Cyr<sup>4</sup>, Eve Galimany<sup>1,2</sup>, Ricardo Santos-Bethencourt<sup>1,2</sup>, Jordi Isern-Fontanet<sup>1,2</sup>,

4 Jordi Ribera-Altimir<sup>1,2,3</sup>, Joan Sala-Coromina<sup>1,2,3</sup>, Mariona Panisello-Garriga<sup>1,2</sup>, Joan B. Company<sup>1,2</sup>

5

6 <sup>1</sup> Catalan Institute of Research for the Governance of the Sea (ICATMAR), Passeig Marítim de la Barceloneta  
7 37-49, 08003 Barcelona, Catalonia, Spain.

8 <sup>2</sup> Institute of Marine Sciences (ICM-CSIC), Passeig Marítim de la Barceloneta 37-49, 08003 Barcelona,  
9 Catalonia, Spain.

10 <sup>3</sup> Department of Earth and Ocean Dynamics, Facultat de Ciències de la Terra, Universitat de Barcelona, Martí  
11 i Franqués, s/n, 08028 Barcelona, Catalonia, Spain.

12 <sup>4</sup> Centre for Fisheries Ecosystem Research, Fisheries and Marine Institute of Memorial University, 155 Ridge  
13 Road, St. John's, Newfoundland and Labrador, A1C 5R3, Canada.

14

15 *Correspondence to:* Mireia G. Mingote ([mireiag@icm.csic.es](mailto:mireiag@icm.csic.es)).

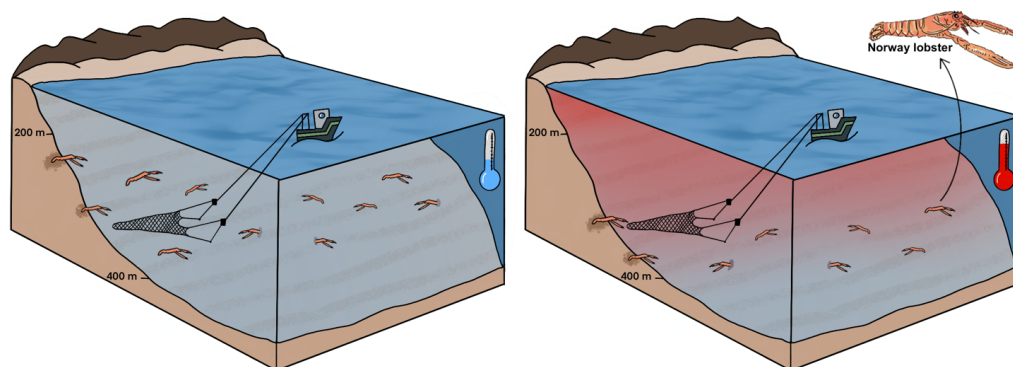
16



17 **Abstract**

18 Understanding how environmental variability shapes the dynamics of demersal resources is essential for  
19 sustainable fisheries management in climate-sensitive regions such as the Northwestern Mediterranean Sea.  
20 This study analyses more than five decades (1970–2024) of Norway lobster (*Nephrops norvegicus*) landings  
21 in FAO GSA 6 to identify the drivers underlying its decadal variability and the sharp decline observed since the  
22 mid-2010s. Fishery-dependent data (landings, Landings Per Unit of Effort (LPUE), depth distribution, and  
23 fishing effort) was combined with oceanographic descriptors. Empirical Orthogonal Functions (EOFs) were  
24 applied to temperature, salinity, along-shore and across-shore currents at surface, 200 m, 400 m, and 600 m  
25 to extract dominant modes of oceanographic variability and assess their correlation with fisheries indicators.  
26 The most relevant physical signal was a widespread warming and salinization of intermediate waters, captured  
27 within its EOF first modes, that showed the strongest negative correlation with landings and LPUE. Positive  
28 phases of these modes corresponded to positive thermal and salinity anomalies and coincided with declining  
29 LPUE, a slight deepening of its centroid (depth of maximum LPUE), and reduced landings. These results  
30 indicate that intermediate-water warming and salinization might be a key mechanism constraining the Norway  
31 lobster catchability. Circulation changes also seemed to influence LPUEs. The second EOF mode of  
32 along-shore velocity at 200 m captured variability in the Liguro-Provençal-Catalan current and the North  
33 Balearic Front. Its positive phases, reflecting a strengthened boundary current and enhanced recirculation  
34 north of the Balearic Islands, were positively correlated with landings, suggesting that frontal dynamics may  
35 modulate habitat suitability, for example. Overall, the recent decline of the Norway lobster landings cannot be  
36 attributed to fishing effort alone but is also linked to climate-driven changes in intermediate-water physical  
37 characteristics. These findings highlight the need to integrate oceanographic indicators into stock assessments  
38 to anticipate further climate-induced shifts in demersal resources.

39





40 **Keywords**

41 Climate fluctuations

42 Demersal fisheries

43 EOFs (Empirical Orthogonal Functions)

44 Fishery-dependent data

45 Fisheries environment

46 *Nephrops norvegicus*



47 **1. Introduction**

48 The ocean climate naturally fluctuates on different temporal scales (Munn, 2002). Climate variability derived  
49 from anthropogenic activity is causing an additional stress to the marine environment as a consequence of  
50 ocean warming, acidification, changes in primary production, oxygen concentration and circulation, among  
51 others (Chust et al., 2024; Rhein et al., 2013). Marine species are sensitive to climate change at both organism  
52 and population level, meaning that they are directly influenced by the changing environment around them,  
53 which they compensate by colonizing new territories (Pinsky et al., 2020). This is causing a rapid redistribution  
54 of marine species (Pecl et al., 2017; Pinsky et al., 2020), causing them to move towards the poles, deeper  
55 waters, or other directions searching for environmental conditions more suitable for their biological needs  
56 (Chen et al., 2011; Parmesan & Yohe, 2003; Perry et al., 2005). Climate change is not only altering the  
57 distribution of the species but also their abundance causing, for example, tropicalization or deborealization,  
58 that is an increasing abundance of warm-affinity species or decreasing abundance of cold-affinity species  
59 (McLean et al., 2021; Zarzychny et al., 2024). These effects are occurring globally, but not uniformly, and they  
60 become especially relevant in some regions considered “hotspots” for climate change (Bilbao et al., 2019),  
61 such as the Mediterranean Sea (Giorgi, 2006).

62

63 The Mediterranean Sea is a semi-enclosed basin with an overall cyclonic density-driven circulation where deep  
64 convection occurs (Millot & Taupier-Letage, 2005). The residence time of its waters is 10 times shorter than  
65 those of the global ocean (Durrieu de Madron et al., 2011) and the response to weather-related stress is  
66 amplified (Cacho et al., 2002). The Mediterranean Sea is thus a key region to observe the effects of climate  
67 change. Warming and salinization of the Mediterranean Sea has been reported in many studies (Adloff et al.,  
68 2015; Margirier et al., 2020; Schroeder et al., 2017). For example, temperature has increased at rates of  
69 0.35°C–0.37°C per decade over the last 40 years (Pastor et al., 2020; Pisano et al., 2020). These  
70 environmental trends alter the marine-community composition, and can lead to changes in fisheries' catch  
71 composition (i.e. tropicalization of the catch, Vergés et al., 2014), affecting the fishing resources and the  
72 socioeconomics of the sector (Perry et al., 2005; Pinsky et al., 2021). In the Northwestern (NW) Mediterranean  
73 Sea, the deep-water rose shrimp, *Parapenaeus longirostris* (Lucas, 1846), expanded northwards and  
74 increased its abundance becoming one of the most caught species by the bottom-trawling fleet in the recent  
75 years (ICATMAR, 2025; Mingote et al., 2024). High climate variability in Mediterranean waters has favored  
76 this species distribution, but these environmental changes may affect other target species differently. This may



77 be the case of the Norway lobster, *Nephrops norvegicus* (Linnaeus, 1758), that has experienced a decline in  
78 catches in the last decade in the NW Mediterranean (ICATMAR, 2025; Vigo et al., 2024).

79

80 The Norway lobster is a benthic decapod crustacean found in the northeastern Atlantic Ocean and in the  
81 central-western Mediterranean Sea, inhabiting muddy bottoms at depths from 20 to 800 meters across a wide  
82 range of environmental conditions (FAO, 2025). In the Mediterranean Sea, populations are mainly found on  
83 the upper slope, between depths of 300 and 600 m (Abelló et al., 2002; Maynou & Sardà, 1997). The species  
84 is described to tolerate temperatures between 6.4 and 17.3 °C, oxygen concentrations ranging from 5.9 to 9.4  
85 mg O<sub>2</sub> mg L<sup>-1</sup>, and salinity levels between 31.8 and 38.8 g Kg<sup>-1</sup> (Johnson et al., 2013), being also influenced  
86 by the seasonal and diel (day/night) cycles (Aguzzi et al., 2003). These effects may vary with depth, where  
87 light intensity is reduced (Aguzzi et al., 2009), affecting populations and their behavior. Environmental  
88 conditions may play a key role in influencing hatching and larval settlement, and consequently their catch.  
89 Global catches of the Norway lobster have been reported since 1980 with a total worldwide of 50,869 t in 2023,  
90 making it one of the most valuable fisheries in all European waters (FAO, 2025). In the NW Mediterranean  
91 Sea, this fishery resource, mainly fished by bottom trawlers together with other species (Sardà, 1998), has lost  
92 importance both in landings and revenues between 2008 and 2024, with a reduction of 57% and 50%,  
93 respectively (ICATMAR, 2025). Moreover, total annual catches have been surpassed by other species that 10  
94 years ago were not present in catches, such as the blue crab, *Callinectes sapidus*, or by other species whose  
95 landings have increased exponentially, such as the deep-water rose shrimp.

96

97 In 2018, the European Union (EU) implemented the Western Mediterranean Multi-Annual Plan (WMMAP)  
98 through regulation COM/2018/0115 final - 2018/050 (COD), aiming to promote sustainable fishing and secure  
99 associated economic, employment, and social benefits. In the NW Mediterranean, the WMMAP covers the  
100 most commercially important demersal species (i.e., the red mullet, the European hake, the deep-water rose  
101 shrimp, the Norway lobster, and the blue and red shrimp), providing a framework for their sustainable  
102 management. Considering its importance as a fishery resource and the observed reduction in catches in recent  
103 years, the aim of this work was to determine the factors driving the fluctuations in Norway lobster catches over  
104 more than 50 years (i.e., 1970-2024) and the declining trend observed in the last 10-15 years in the Food and  
105 Agriculture Organization (FAO) Geographical Subarea 6 (GSA 6). This work evaluates the time series of  
106 landings and Landings Per Unit of Effort (LPUE) of the Norway lobster, including its distribution in depth. Then,  
107 fishing effort and environmental variables are examined and correlated to landings and LPUE trends.



108 **2. Materials and methods**

109 **2.1. Study area**

110 The study area considers the NW Mediterranean Sea, focusing on fishery-dependent data from the GSA 6

111 Fig. 1), which extends from Cape Creus to Cartagena, as defined by the General Fisheries Commission of the

112 Mediterranean (GFCM; EU 1343/2011; Resolution GFCM/33/2009/2).

113

114

115

116

117

118

119

120

121

122

123

124

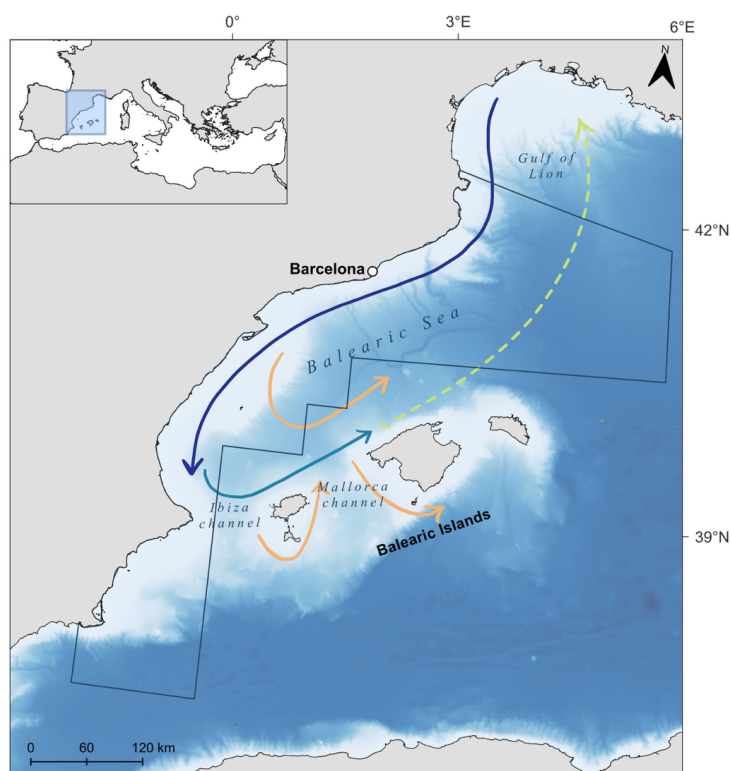
125

126

127

128

129



130

131

132

133

134

135

136

137

138

Figure 1. Study area indicating the geographical limits of the GSA 6. Surface currents are indicated in different colors: Liguro-Provençal-Catalan current, in solid blue; recirculation in solid light blue; North Balearic front in dashed light green; permanent path in solid orange. Information adapted from Millot & Taupier-Letage (2005).

An important oceanographic feature of the NW Mediterranean Sea is the Liguro-Provençal-Catalan current also known as “Northern Current” (Castellón et al., 1990). This current originates in the Ligurian Sea and flows southwestward along the northern edge of the NW Mediterranean Sea while receiving input from major rivers. As the Liguro-Provençal-Catalan current reaches the end of the Balearic Sea and the shallower ridge created by the Balearic Islands, a fraction of the current retroflects northwestward along the northern sides of the



139 islands, while other fractions continue south through Ibiza and Mallorca channels (Fig. 1; see also Balbín et al.,  
140 2014). This general circulation creates two main density fronts. While the Catalan front is associated with  
141 strong salinity gradients created by the Liguro-Provençal-Catalan current, the Balearic front is formed by  
142 temperature gradients between the cooler retroflection and the warm waters surrounding the Balearic Islands.  
143 In the central area of the Balearic Sea between those two frontal systems, instabilities generated by cyclonic  
144 eddies keep the stratification weak (Font et al., 1988).

145

## 146 **2.2. Dataset**

### 147 **2.2.1. Landings and Landings Per Unit of Effort time series**

148 Data on the Norway lobster landings from 1970 to 1986 were obtained from the official Spanish Fishing  
149 Statistics (*Estadística de Pesca*) and Yearbook of Maritime Fishing (*Anuario de Pesca Marítima*) from the  
150 *Subsecretaría de la marina mercante* later called *Subsecretaría de pesca y marina mercante* of the Spanish  
151 Government. The Spanish annual demersal landings statistics were collected from 1933 to obtain national  
152 information on landings and effort for statistical purposes, but the compilation stopped in 1986 after the entry  
153 of Spain into the European Union (Punzón et al., 2020). In these books, data are aggregated in eight regions  
154 (*Balear, Canaria, Cantabrica, Levantina, Noroeste, Surmediterranea, Suratlántica* and *Tramontana*), with  
155 values provided for the provinces included in each of them. Only data from provinces within the GSA 6 area  
156 were considered for this study, i.e. Girona, Barcelona, Tarragona, Castelló, Valencia, Alacant and Murcia.

157

158 Landing data from 1987 to 2003 were extrapolated to the whole GSA 6 area based on existing landings data  
159 from Catalonia (Martín, 1991) and daily commercial fishing landings provided by the Catalan government  
160 (Department of Climate Action, Food and Rural Agenda). The extrapolation consisted in defining a relation  
161 factor between landings in Catalonia and GSA 6 the years when data were available in both cases (1970-  
162 1986, 2004-2024). For data between 1987 and 1999, the relation factor defined was 1.58 and was calculated  
163 averaging data from 1980 to 1986. For years 2000 to 2003, the relation factor used was 1.29 and was  
164 calculated averaging data from 2004 to 2007. The use of two different relation factors was determined after  
165 evaluating the available trends for Catalonia landings data.

166

167 Data from 2004 to 2024 were obtained from landings of the Spanish Fisheries Secretariat (*Secretaría General*  
168 *de Pesca*, SGP, Spanish Government). As described in Mingote et al. (2024), in the Spanish Mediterranean,  
169 landings are sold fresh daily at the fishing auctions, providing information on the economic value and the total



170 kg by each landed species. These data are gathered by the SGP and later processed by the Catalan Institute  
171 of Research for the Governance of the Sea, ICATMAR (ICATMAR, 2025; Ribera-Altimir et al., 2023) for the  
172 GSA 6 region. Finally, the landing time series for the three periods (1970-1986, 1987-2003, and 2004-2024)  
173 were merged into a single dataset.

174

175 For obtaining LPUE time series from 2008 to 2024, we followed the procedure described in Mingote et al.  
176 (2024) and briefly summarized here. Vessel Monitoring System (VMS) data for the trawling fleet were analyzed  
177 following the methodology described in Sala-Coromina et al. (2021) for obtaining information on georeferenced  
178 vessel hauls and fishing time in hours. Then, VMS and landing data were joined resulting in a dataset with  
179 information on the Norway lobsters' landings and total fishing time for each vessel fishing haul. Then, the  
180 variables were aggregated yearly for the whole fleet in a 1 km<sup>2</sup> grid (EPSG 4326) on the GSA 6 area, enabling  
181 the calculation of LPUE (kg h<sup>-1</sup> km<sup>-2</sup>) averaged per year.

182

### 183 **2.2.2. Fishing effort trend**

184 Fishing efforts from 2004 to 2024 were estimated using data on the number of fishing trips and vessels  
185 operating in the bottom-trawl fleet. In the study area, vessels operate in the vicinity of each port and land their  
186 catch daily (Carreton et al., 2025). Accordingly, a fishing trip, also referred to as a fishing day, is defined as  
187 the period between a vessel's departure from port and its return, occurring within the same day. Fishing trips  
188 are identified using a unique vessel identifier and the date of the activity. Information on both the number of  
189 vessels from the bottom-trawl fleet in the GSA 6 area, and the fishing trips conducted was obtained from the  
190 SGP landings database.

191

### 192 **2.2.3. LPUE depth distribution and centroid depth**

193 LPUE data were associated with bathymetric data obtained from the General Bathymetric Chart of the Oceans  
194 (GEBCO) portal, with a spatial resolution of 15 arcsec (GEBCO Compilation Group, 2024). Depth values were  
195 extracted from the bathymetry shapefile and joined with georeferenced LPUE (1 km<sup>2</sup> grid described above) to  
196 obtain the depth of each grid point. Data were aggregated by year and depth for representing the distribution  
197 of averaged LPUE values in depth. Then, the centroid depth, or average depth where most of the LPUE occurs,  
198 was calculated yearly following this formula:

199

$$\text{Centroid depth} = \frac{\sum_i (LPUE_i \cdot z_i)}{\sum_i LPUE}$$



200 where  $\Sigma_i$  refers to a sum on all 1 km<sup>2</sup> pixels with LPUE values for a certain year (LPUE<sub>i</sub>), and  $z_i$  refers to the  
201 depth of the sea floor at that location (i.e., where the fishing occurs).

202

#### 203 **2.2.4. Environmental data**

204 Monthly fields of the Mediterranean Sea Physics Reanalysis (Escudier et al., 2020, 2021; Nigam et al., 2021)  
205 were extracted from the Mediterranean Forecasting System (MFS) openly available on the Marine Data Store  
206 of the E.U. Copernicus Marine Environment Monitoring Service (CMEMS). The model has a horizontal grid  
207 resolution of 1/24° (ca. 4-5 km) and 141 unevenly spaced vertical levels. Temperature and salinity vertical  
208 profiles as well as and along track satellite Sea Level Anomaly observations are assimilated in the model. The  
209 core reanalysis product covers the period 1987-01-01 to 2025-12-01. Then, data for the NW Mediterranean  
210 Sea were extracted, here defined as the region between [36.06, 43.87] °N and [-1.84, 7.27] °E, for the complete  
211 time series between 1987 and 2024.

212

#### 213 **2.3. Analyses**

214 Empirical Orthogonal functions (EOFs) is a type of Principal Component Analysis (PCA) commonly used in  
215 Earth Sciences to decompose complex spatio-temporal signals into a finite set of dominant spatial patterns  
216 (Hannachi et al., 2007). EOFs are by essence a statistical exploratory method and in consequence the  
217 resulting components and scores may not always be meaningful from a mechanistic point of view. They are  
218 however a powerful tool often used in atmospheric and ocean sciences to extract patterns of variability that  
219 may be otherwise hidden under multiple complex interactions.

220

221 In this study, EOFs were performed using the Python package *xeofs* (Rieger & Levang, 2024). EOFs were  
222 applied on Temperature, Salinity and Currents from discrete depth levels. All fields were linearly de-trended  
223 before applying the EOFs to remove any long-term trends attributable, for example, to anthropogenic climate  
224 change. We selected the closest depth level from the model data to surface, 200 m, 400 m and 600 m. These  
225 depths were chosen to cover the optimal depth for the Norway lobster, or the depth range where the species  
226 is caught, and to help us understand any relevant oceanographic process. Ocean currents (East and North)  
227 were also rotated by -210°, which is equivalent to a 210° anticlockwise rotation of the axis system, so the x-  
228 axis matches the flow direction of the Catalan Current (U positive southwestward along shore, and V positive  
229 southeastward across shore).



230

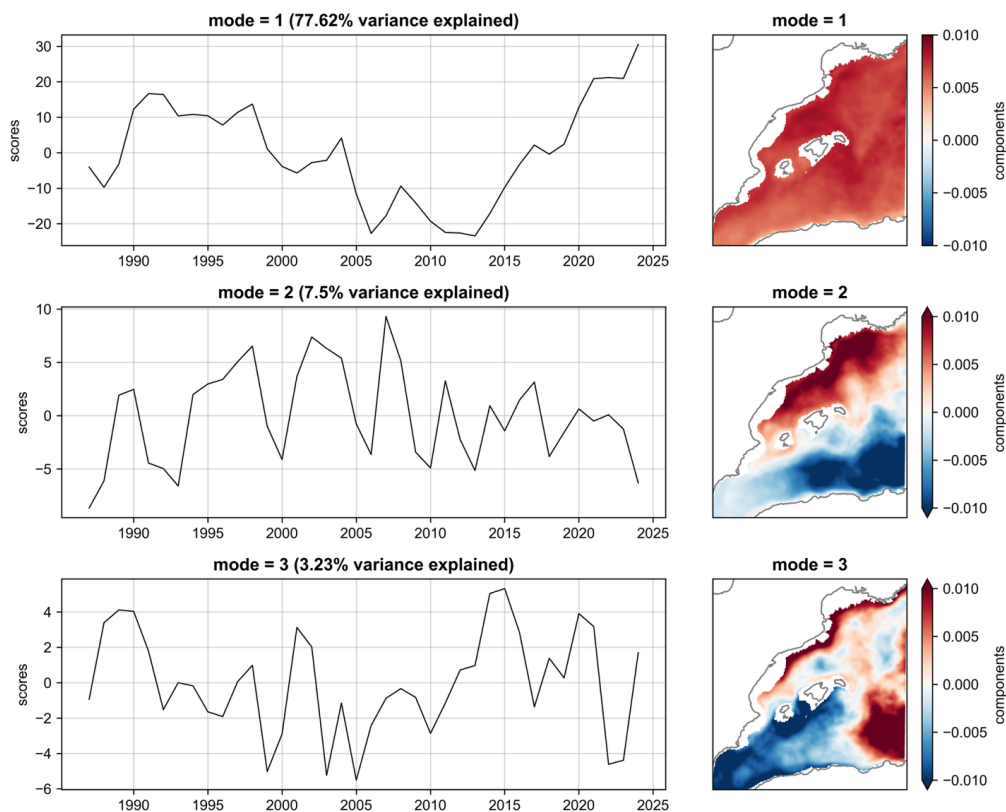
231 The EOF analysis decomposes a spatiotemporal signal into a series of orthogonal (i.e. independent) modes,  
232 each explaining a decreasing fraction of the variance of the original signal. Each mode comprises a component  
233 (spatial maps of variance) and a time-varying score (how the component varies in time). Ultimately, the original  
234 signal could be re-constructed by adding each mode together.

235

236 To better explain the interpretation of the EOFs, temperature at 400 m is used as an example (Fig. 2). Mode  
237 1, the dominant pattern, explains approximately 78% of the variance. It is characterized by a near-  
238 homogeneous spatial pattern, with all the region colored in red (positive values, Fig. 2), associated with a  
239 temporal variability representing decadal cycles over the period studied. This can be interpreted as a  
240 widespread increase or decrease in temperature on annual time scales. Mode 2 and 3 represent faster  
241 fluctuating temporal signals, with more than 7% and 3% of the variance explained, respectively (Fig. 2). These  
242 modes represent inter-annual oscillations in temperature at smaller regional scales compared to the  
243 widespread mode 1. For example, mode 2 spatial pattern presents two well-distinguished areas: northern area  
244 (Balearic Sea) positive, and southern (Central NW Mediterranean south of the Balearic Islands) negative. This  
245 means that when the temporal pattern scores are positive, the expression of this mode is characterized by  
246 warmer temperatures north of the Balearic Islands, and colder temperatures in the south. This mode possibly  
247 relates to a local process of temperature changes with an inshore/offshore component. Mode 3 is similar to  
248 mode 2, with three well-distinguished areas, representing an even more local process. Overall, mode 2 and 3  
249 remain marginal compared to mode 1 that explains more than 10 times more variance.

250

251 The decomposition procedure was repeated for all variables and depths considered in this study and the three  
252 leading modes for each of the 16 combinations (i.e., 4 variables at 4 depths) are provided in the Appendices.  
253 Then the resulting scores were all cross correlated (16 x 3 modes = 48) with the landings and LPUE time  
254 series. The environmental time series best correlated with the fisheries data were selected for further analysis  
255 in Sect. 3.



256 Figure 2. EOFs of the three first modes of variability for the de-trended annual temperature at 400 m between 1987 and  
257 2024. The EOF components (spatial correlation maps) are shown on the right panels, with the scores (temporal variability  
258 of the components) on left panels. The percentage of the variance explained by each mode is also shown on top of the left  
259 panels. Here, positive score values indicate increasing temperature in areas where the spatial correlation is positive (red  
260 on the maps).



### 261 3. Results

#### 262 3.1. Variability of the Norway lobster time series

263 Total yearly landings (t) of the Norway lobster were plotted together with LPUE ( $\text{kg h}^{-1} \text{km}^{-2}$ ) and centroid depth  
264 (m) from 1970 to 2024 (Fig. 3). During this period, total landings presented large decadal fluctuations. Landings  
265 between 1970 and 1998 remained relatively low, oscillating between 217 and 366 t, only with a peak value of  
266 435 t in 1977. Between 1999 and 2014, landings presented an increasing trend, reaching the maximum value  
267 of all the time series of 568 t in 2012. From 2015 onwards, the landings decreased and reached their lowest  
268 level of the time series of 185 t in 2023. The difference between the highest and lowest peak represents a  
269 reduction of 67% in Norway lobster landings in 11 years. Total landings and LPUE from 2008 to 2021 presented  
270 similar trends (Fig. 3). That is, between 2008 and 2012, LPUE followed an increasing pattern, reaching its  
271 highest peak of  $0.9 \text{ kg h}^{-1} \text{km}^{-2}$  also in 2012. From 2013 to 2023, LPUE was reduced by almost 58%, reaching  
272 the lowest value of  $0.4 \text{ kg h}^{-1} \text{km}^{-2}$  in 2021.



273 Figure 3. Historical series of total yearly landings of the Norway lobster from 1970 to 2024 (solid black line, t); yearly  
274 average LPUE from 2008 to 2024 (solid blue line,  $\text{kg h}^{-1} \text{km}^{-2}$ ); and yearly centroid depth from 2008 to 2024 (solid red line,  
275 m). All landing data correspond to the GSA 6 area.

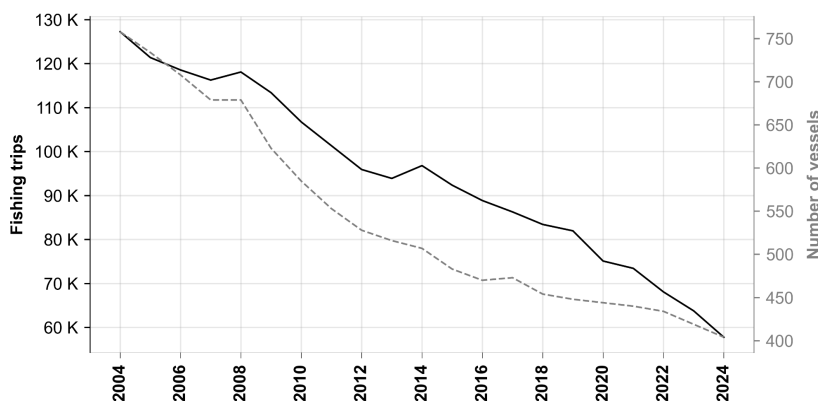
276

#### 277 3.2. Variability of fishing effort

278 The total number of fishing trips and vessels in the bottom-trawl fleet showed a consistent declining trend  
279 between 2004 and 2024 (Fig. 4). Over this period, the bottom-trawl fleet operating in the GSA 6 area was  
280 reduced by 47%, decreasing from 758 vessels in 2004 to 404 in 2024. A similar pattern was observed with the  
281 number of fishing trips, which declined by 55%. This reduction in fishing trips is directly linked to the diminution  
282 of the fleet, as fewer vessels conducted fewer fishing operations.



283  
284  
285  
286  
287  
288  
289  
290  
291  
292



293 Figure 4. Time series of fishing trips (solid black line) and number of bottom-trawlers (dashed grey line) from 2004 to 2024  
294 within the GSA 6 area.

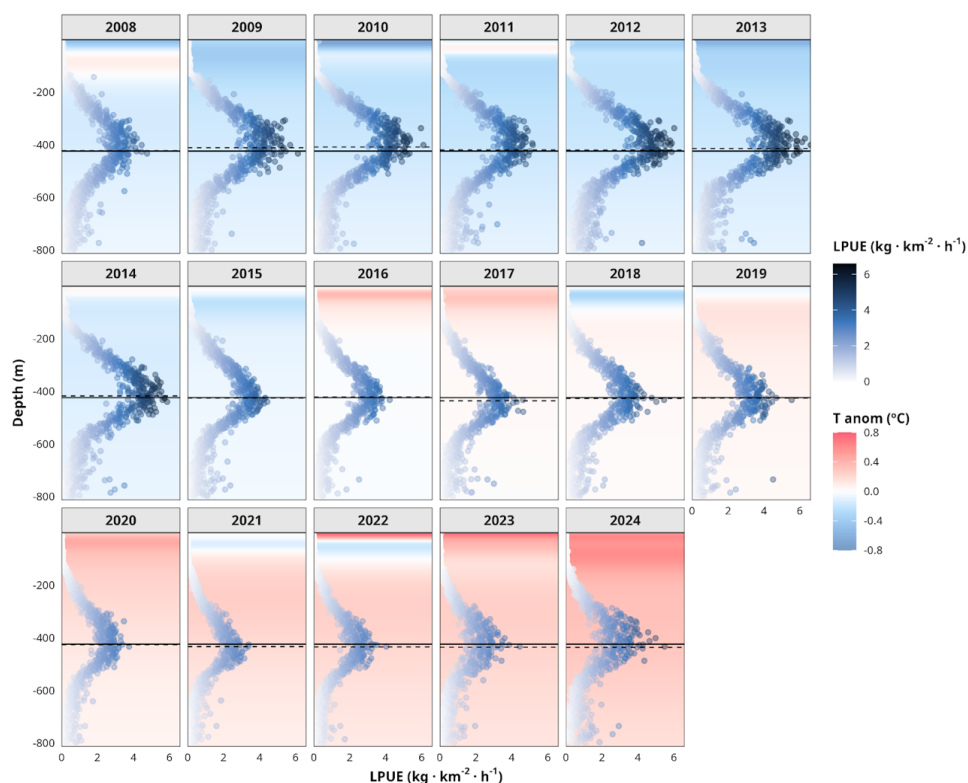
295

296 **3.3. Distribution of the Norway lobster LPUE and temperature anomaly in depth**

297 The centroid depth between 2008 and 2024 followed a fluctuating but with an increasing trend (i.e., deeper  
298 depths; Fig. 3). Depths for the maximum LPUE during this period oscillated between a minimum of 410 m and  
299 a maximum of 435 m reached in 2010 and 2024, respectively. The trend observed here outlines a general  
300 pattern of higher values of LPUE are obtained when fishing occurs in shallower areas while lower LPUE are  
301 associated with fishing in deeper areas. This suggests that as the average LPUE declines, the maximum LPUE  
302 are found at deeper depths, and vice-versa.

303

304 The annual vertical distribution of LPUE averaged over GSA 6 between 2008 and 2024 and its relation to the  
305 temperature anomalies (°C) is shown in Fig. 5. The yearly centroid depth (from Fig. 3) is also added to this  
306 figure (horizontal dashed lines), together with its average over the time series (horizontal solid lines). In the  
307 period examined, LPUE follow a pattern of higher values around 400 m depth that decrease at shallower and  
308 deeper depths. This trend indicates the depths where the LPUE mainly concentrates. The maximum LPUE  
309 was achieved in 2013, with 6.6 kg h<sup>-1</sup> km<sup>-2</sup> at 401 m depth. Then, values decreased but were concentrated  
310 around similar depths. In detail, centroid depths changed a few meters in the time series, as shown in Fig. 5,  
311 with a general pattern of higher depths coinciding with lower LPUE values. This also matches with a tendency  
312 of positive anomalies of temperature in the water column that started in 2016 and accentuated between 2020  
313 and 2024. This suggests that the recent reduction of LPUE and its shift to greater depths also correspond to  
314 increase in temperature.



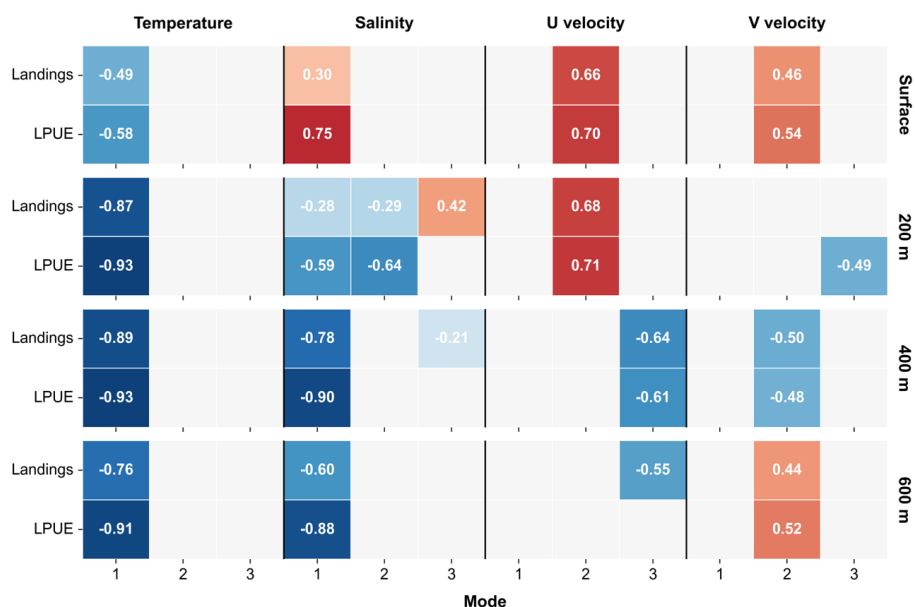
315 Figure 5. Depth distribution of LPUE ( $\text{kg h}^{-1} \text{km}^{-2}$ ) of the Norway lobster and temperature anomaly ( $^{\circ}\text{C}$ ) from 2008 to 2024.

316 Temperature reanalysis data were extracted from the Marine Data Store of the E.U. Copernicus Marine Environment  
 317 Monitoring Service (CMEMS). Solid black line represents mean centroid depth of LPUE, at 424 m; dashed black line  
 318 represents yearly centroid depth of LPUE. All data correspond to the GSA 6 area.

319

320 **3.4. Cross-correlations between environmental descriptors and the Norway lobster landing**  
 321 **time series**

322 The EOF scores of the environmental variables across different depth strata were correlated with the time  
 323 series for landings and LPUE of the Norway lobster. The resulting cross-correlation matrix (Fig. 6) shows that  
 324 landings of the Norway lobster are anti-correlated with the respective scores for temperature at 200, 400 and  
 325 600 m depth ( $T_{200}$  [1],  $T_{400}$  [1],  $T_{600}$  [1]; the number in bracket indicates the mode), salinity at 400 and 600 m  
 326 depth ( $S_{400}$  [1],  $S_{600}$  [1]), and correlated with the scores of along-shore velocity at surface and 200 m depth  
 327 ( $U_{\text{surf}}$  [2],  $U_{200}$  [2]). The highest correlation value is with  $T_{400}$  [1], with a Pearson coefficient value of -0.89. On  
 328 the other hand, the LPUE presents correlation and anti-correlation values similar to those with landings, but  
 329 reaching stronger Pearson coefficient values, such as -0.93 also with  $T_{200}$  [1] and  $T_{400}$  [1].



330 Figure 6. Cross-correlation matrix between landings (t) of Norway lobster from 1970 to 2024, LPUE ( $\text{kg h}^{-1} \text{km}^{-2}$ ) from 2008  
 331 to 2024, and output for the annual, de-trended, spatial modes 1 to 3 of EOFs on reanalysis and forecast temperature,  
 332 salinity, along-shore velocity (U), and cross-shore velocity (V) data from 1987 to 2024 at surface, 200 m, 400 m and 600  
 333 m depth. Landings and LPUE data correspond to the GSA 6. Only significant ( $p\text{-value} < 0.05$ ) Pearson correlation  
 334 coefficients are shown in the matrix, with positive correlations in red and negative correlations values in blue. Darker colors  
 335 indicate stronger correlations.

336 Following the cross-correlation analysis (Fig. 6), a subset of meaningful time series was selected for further  
 337 analysis. These were chosen based on scientific interpretation of the results (Table 1). For example, because  
 338 maximum LPUE of the Norway lobster were mostly between 200 and 400 m (Fig. 5), EOFs at 400 m were  
 339 prioritized for further analysis when the correlation was strong with different depth ranges (e.g. landings are  
 340 anti-correlated with temperature at 200 m, 400 m and 600 m). Following this reasoning, temperature and  
 341 salinity at 400 m and along-shore velocity at 200 m were selected because they all have high correlation with  
 342 landings and represent a meaningful depth range for the Norway lobster’s LPUE. Along-shore velocities at  
 343 surface were also selected because they are highly correlated with the landings, while being potentially  
 344 indicative of changes in the path of the Liguro-Provençal-Catalan current in the area. The selected modes for  
 345 each environmental variable are shown in Fig. 7 to understand better the meaning of their spatiotemporal  
 346 pattern.  
 347



348 Table 1. Summary of the selected EOF outputs for the analyses and their Pearson correlation coefficient ( $r$ ) with landings  
 349 and LPUE. T<sub>400</sub> corresponds to temperature at 400 m depth; S<sub>400</sub> corresponds to salinity at 400 m depth; U<sub>surf</sub>  
 350 corresponds to along-shore velocity at surface; U<sub>200</sub> corresponds to along-shore velocity at 200 m depth. A short  
 351 interpretation is provided along with each correlation. Variables are ordered from highest to lowest percentage of variance  
 352 explained and correlation value. All Pearson correlation coefficients shown are significant ( $p$ -value  $\leq 0.001$ ).

353

354

355

356

357

358

359

360

361

362

EOF	Mode (%var)	Corr w/ landings	Corr w/ LPUE	Interpretation
T <sub>400</sub>	1 (78%)	-0.89	-0.93	Landings/LPUE decrease when widespread temperature at 400 m increases
S <sub>400</sub>	1 (68%)	-0.78	-0.90	Landings/LPUE decrease when widespread salinity at 400 m increases
U <sub>surf</sub>	2 (10%)	0.66	0.70	Landings/LPUE decrease when velocity at surface in the Liguro-Provençal-Catalan current decreases
U <sub>200</sub>	2 (8%)	0.68	0.71	Landings/LPUE decrease when velocity at 200 m in the Liguro-Provençal-Catalan current decreases

363

**3.5. Description of the selected EOF modes**

364 The first EOF mode of temperature at 400m, T<sub>400</sub> [1], explains nearly 78% of the variance (Fig. 7a). In periods  
 365 when the score values are positive (e.g., the 1990s and after 2020), the annual temperature throughout the  
 366 region is above average (higher temperatures). Conversely, the periods with negative scores (e.g. mid-2000s  
 367 to mid-2010s) have a temperature at 400 m below average (lower temperatures). As mentioned in Sect. 2.3,  
 368 this mode corresponds to a widespread increase or decrease of temperature affecting the entire NW  
 369 Mediterranean Sea on near-decadal time scales and is likely reflective of changes in the mean climate over  
 370 the region.

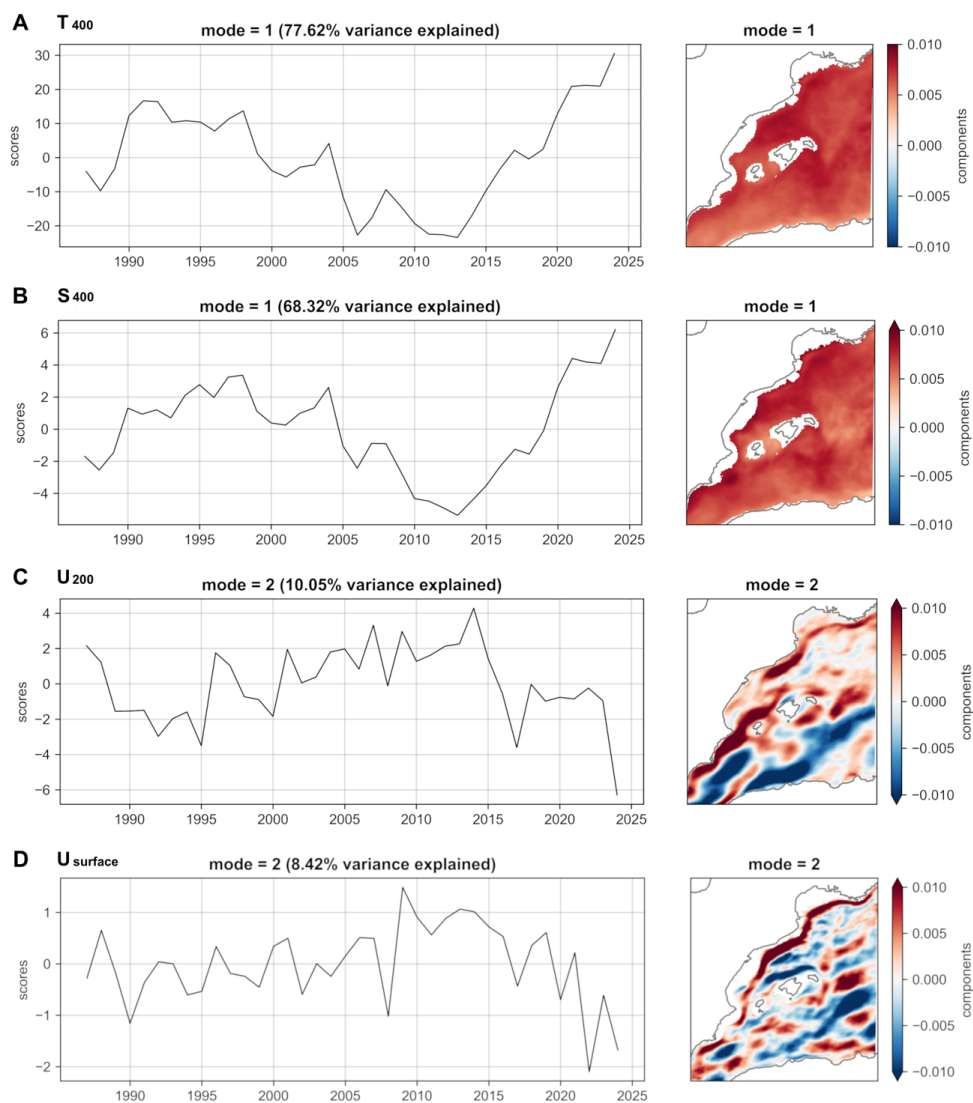
371

372 The first EOF mode of salinity at 400m, S<sub>400</sub> [1], explains around 68% of the variance (Fig. 7b). It follows a  
 373 similar spatiotemporal pattern to temperature, also characterized by annual widespread increase or decrease  
 374 on its values. This indicates that positive phases of the score are associated with periods of increased salinity  
 375 at 400 m.

376



377 Cross-shore velocity at surface and 200m,  $U_{surf}$  [2] and  $U_{200}$  [2], explain approximately 10% and 8% of the  
378 variance, respectively (Fig. 7c, 7d). We note that mode 1 for these two signals only explains a slightly greater  
379 portion of the variance (both approximately 17%), but the component signal in this case is stronger in the  
380 Alboran Sea and south of the Balearic islands, while mode 2 shows a stronger signal in the Balearic Sea and  
381 in the region of interest (GSA 6) in the vicinity of the Liguro-Provençal-Catalan current. This is especially true  
382 for  $U_{200}$  (Fig. 7d) for which a strong spatial signal extending from the Gulf of Lion to the coast of Catalonia is  
383 found along the path of the Liguro-Provençal-Catalan current (red in the figure). For the same component, a  
384 band of negative correlation (blue), is found immediately north of the Balearic Islands, which may be interpreted  
385 as a recirculation current eastward as part of the Balearic front (we recall that the  $U$  current is positive  
386 southwestward in the main direction of the current). Overall, the spatial pattern for  $U_{200}$  [2] may be interpreted  
387 as a stronger Liguro-Provençal-Catalan, recirculation and Balearic front when the score is high (late 2000s  
388 and early 2010s) and a weaker current, recirculation and front when the score is low (in the 2020s).  
389



390 Figure 7. Meaningful EOF modes selected for the analysis. (a) Mode 1 for temperature at 400 m depth; (b) Mode 1  
 391 salinity at 400 m depth; (c) Mode 2 for along-shore velocity at surface; (d) Mode 2 for along-shore velocity at 200 m depth.  
 392 The EOF components (spatial correlation maps) are shown on the right panels, with the scores (temporal variability of the  
 393 components) on left panels. The percentage of the variance explained by each mode is also shown on top of the left  
 394 panels.



395           **3.6. Relation between the selected EOF modes and the Norway lobster time series**

396 Temporal patterns of  $T_{400}$  [1] and  $U_{200}$  [2] were selected to compare with landings of the Norway lobster (Fig.  
397 8a, 8b, respectively). The selected modes for salinity and along-shore velocity at surface were not considered  
398 for the comparison because they presented either similar or less distinguished patterns with the other  
399 variables. The temporal patterns of both environmental variables were also compared (Fig. 8c). The selection  
400 of landings instead of LPUE for the comparison is due to the availability of larger data time series, and because  
401 both parameters have similar high correlation values with the environmental variables evaluated.

402

403 During the period evaluated, landings followed an inverse pattern than  $T_{400}$  [1], with the highest values of  
404 landings correspond to the lowest score values of temperature and salinity at 400 m depth, and vice-versa  
405 (Fig. 8a). Because an increase in  $T_{400}$  [1] scores translates into a widespread increase in temperature (and  
406 salinity for  $S_{400}$  [1]) across the region (Fig. 7a, 7b), a negative correlation with the landings means a decrease  
407 in landings of the Norway lobster when temperature and salinity increase (Table 1, Fig. 8).

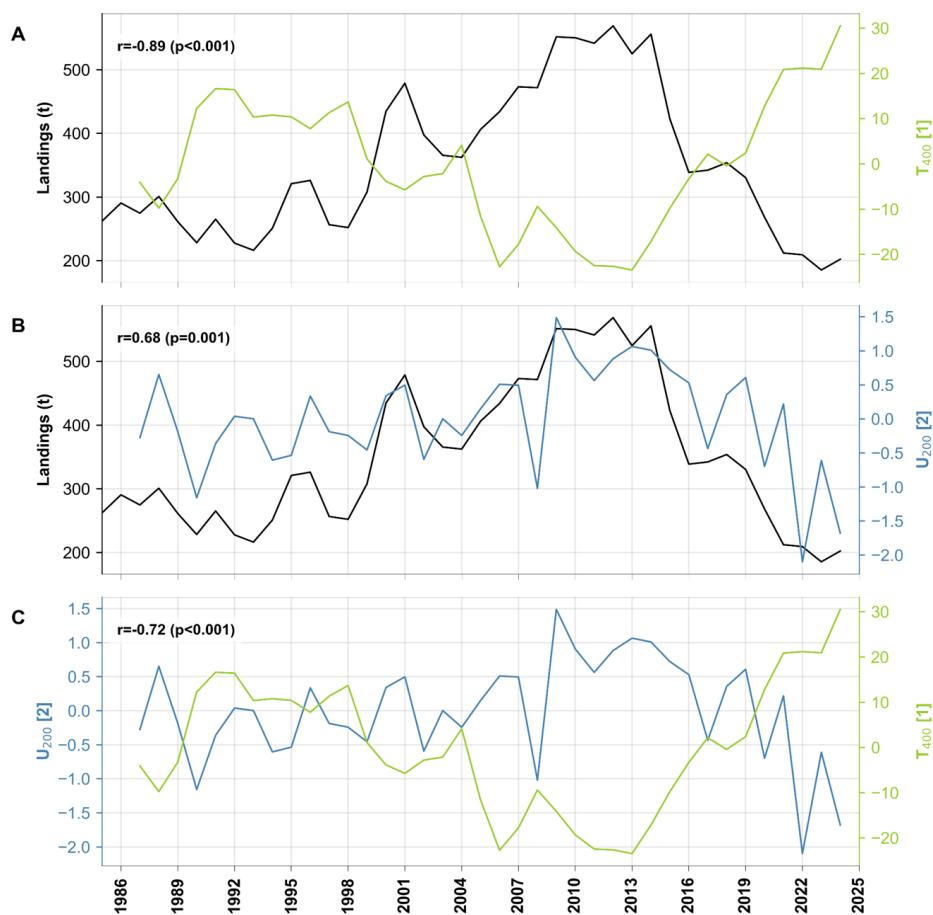
408

409 Landings and  $U_{200}$  [2] followed similar trends, with increasing landings when the score values for  $U_{200}$  [2]  
410 increase too (Fig. 8b). Along-shore velocity at 200 m depth does not follow a homogenous spatial pattern  
411 within all the region, but  $U_{200}$  [2] component shows a strong correlation in the Liguro-Provençal-Catalan current  
412 region (Fig. 7d). This means that a decrease in the Norway lobster landings could be related with an increase  
413 in the velocity of the Liguro-Provençal-Catalan current, and a potential displacement of the North Balearic front  
414 at 200 m depth (Table1, Fig. 8).

415

416  $T_{400}$  [1] is anti-correlated with  $U_{200}$  [2] (Fig. 8c). These inverse patterns suggest that years with a widespread  
417 increase in temperature at 400 m depth are most likely to be associated to a decrease in the velocity of the  
418 Liguro-Provençal-Catalan current velocity and a decrease in the velocity of the recirculation north of the  
419 Balearic Islands at 200 m depth (Fig. 8). This dynamic is explored further in the Discussion.

420



421 Figure 8. Time series of total yearly landings (t) of the Norway lobster (solid black line, t) from 1986 to 2024, and the  
 422 temporal pattern of the selected modes of environmental variables from 1987 to 2024. (a) Comparison between landings  
 423 and  $T_{400}$  [1], corresponding to the mode 1 score values for temperature at 400 m depth (solid green line); (b) Comparison  
 424 between landings and  $U_{200}$  [2] corresponding to the mode 2 score values for along-shore velocity at 200 m depth (solid  
 425 blue line); (c) Comparison between  $U_{200}$  [2] and  $T_{400}$  [1]. Values presented in the y-axis for the environmental variables  
 426 correspond to the score value obtained from the EOFs calculations. The Pearson correlation coefficients (r) and p-values  
 427 between the curves in each plot are shown.

428



429 **4. Discussion**

430 Landings of the Norway lobster in the GSA 6 region (NW Mediterranean Sea) show important fluctuations over  
431 the past 54 years, in addition to a sharp decline in landings and LPUE over the last 15 years. This recent  
432 decline has also been reported in other areas, such as the North and NW Iberian Peninsula or SW Ireland,  
433 where landings of the species decreased by 80-90% in 25 years (Fariña & González Herraiz, 2003; González  
434 Herraiz et al., 2009, 2015). The Norway lobster is a valuable fishing resource and the variability of its landings  
435 and catchability rely partially on the efficiency of the fishing gear, the accessibility of the fishing grounds and  
436 its vulnerability to the gears (Maynou & Sardà, 2001). Several studies have found depth, atmospheric pressure,  
437 cloud cover, current speed, turbidity and nature of the sediments, among others, to have an effect on the  
438 Norway lobster catch rates (Aguzzi et al., 2003; Chapman & Howard, 1988; Maynou & Sardà, 2001; Newland  
439 et al., 1988; Sardà, 1995; Tuck et al., 1997; Tully & Hillis, 1995). Therefore, the reasons behind those  
440 fluctuations in catches can be diverse and may include environmental and fishing traits. Here, we review  
441 observed fluctuations in Norway lobster catches and LPUE and propose hypotheses to interpret these patterns  
442 in the context of changing environmental conditions and fishing effort.

443

444 **4.1. Reduction of fishing effort**

445 In the Spanish Mediterranean, bottom trawling is restricted to a maximum of 12 fishing hours per day and five  
446 days per week (EC 1626/1994; EC 1967/2006), a regulation aimed at controlling total effort and reducing  
447 pressure on demersal resources. In recent years, under the EU WMMAP framework, fishing effort for the  
448 bottom-trawl fleet has been reduced through limits on days at sea, within a broader context in which the number  
449 of operating bottom-trawl vessels has also declined (MAPA, 2025). This coincides with the most recent period  
450 of a declining trend in Norway lobster catches (Fig. 3, 4). However, the simultaneous decrease observed in  
451 both landings and LPUE suggests that the reduction in landings cannot be explained simply by the reduction  
452 in fishing effort. Even under conditions of fewer vessels and fewer fishing trips, LPUE continue to decline,  
453 indicating a decrease in stock availability or abundance. This pattern may reflect broader ecological or  
454 environmental drivers, such as changes in habitat conditions, recruitment success, or ecosystem dynamics,  
455 which are acting independently of effort reduction and may be limiting the recovery of the Norway lobster stock.

456

457

458



459           **4.2.    Warming temperature, species displacement and changing fishing strategy**

460    Warming of the ocean has been recorded globally since 1880 (NOAA, 2024). In the NW Mediterranean Sea,  
461    higher temperatures have been observed since 2014 (Bahamon et al., 2020; Margirier et al., 2020), matching  
462    the trend observed here at depth for the same period (Fig. 7a, A2a, A3a). This recent warming trend also  
463    corresponds to a decline in LPUE and an increase in the depth at which the maximum LPUE is found (i.e.  
464    LPUE centroid depth; Fig. 3). Overall, this supports the idea that as water temperature warms, the Norway  
465    lobster population is moving deeper. Vertical displacement to reach cooler waters has been reported as a  
466    strategy followed by some species to adapt to ocean warming (Jorda et al., 2020), moving a few meters per  
467    year to keep pace with climate change (Poloczanska et al., 2013). We could hypothesize a shift in the species  
468    vertical distribution to escape environmental conditions that are less suitable for them and, consequently,  
469    fishers changing their fishing strategy or target. In a multispecific fishery, such as the bottom-trawl in the NW  
470    Mediterranean Sea, the diversity of the catch and the mobility of the species can protect the communities from  
471    environmental change effects (Young et al., 2019). For example, the deep-water rose shrimp is another target  
472    species of bottom trawlers at this depth showing an exponential increase of its abundance during the same  
473    period as the decline of the Norway lobster (Mingote et al., 2024). This species became the second most  
474    important fishing resource economically, and the first in weight in the GSA 6 in 2024, potentially offsetting the  
475    loss of revenue caused by the reduction of catches of the Norway lobster (ICATMAR, 2025).

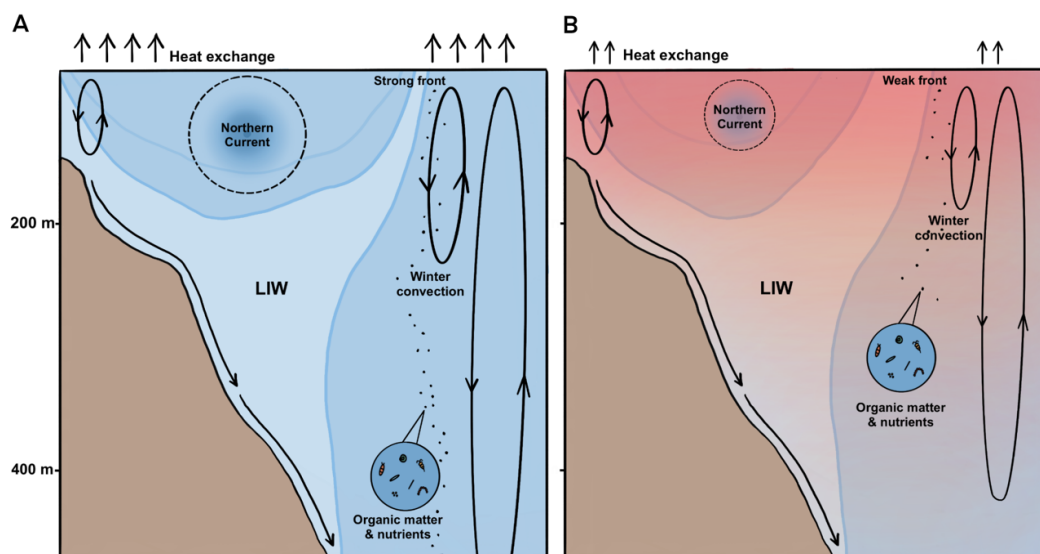
476

477           **4.3.    Large-scale oceanographic changes in the Mediterranean Sea**

478    In this study, we detected a widespread increase in temperature and salinity in the region from surface to 600  
479    m depth (Fig. 5a, 5b, A1-A7a) starting from 2014 up to now. This trend matches with previously reported  
480    warming and salinization of the intermediate and deep layers of the Western Mediterranean (Bahamon et al.,  
481    2020; Margirier et al., 2020). The NW Mediterranean Sea is known for its deep or intermediate convection and  
482    deep-water formation that take place due to winter heat loss and evaporation resulting from cold and strong  
483    northerly winds (Fig. 9a; Puig et al., 2013). Margirier et al. (2020) reported the accumulation of warmer and  
484    more saline Levantine Intermediate Water (LIW) in the northwestern basin until 2018 related to a weak winter  
485    convection in 2014 (Fig. 9b). This phenomenon caused an increase in stratification below the LIW that,  
486    together with the air-sea heat fluxes intensity, constrained the depth of convection. Vertical sinking of organic  
487    material from the euphotic zone is known to be the main source of nutrients to the deep-sea floor, controlling  
488    the dynamics of biological processes (Billett et al., 1983; Gage, 2002). The transport of organic matter to the



489 deep basin thus likely determine the nutritive condition of populations and the reproductive output (Company  
490 et al., 2008). So, the increase in stratification because of warmer and saltier water weaken the convection and  
491 less nutrients arrive to deeper depths, potentially affecting the income of organic matter of benthic populations.  
492  
493 We also found a pattern of change in the intensity of the Liguro-Provençal-Catalan current and the North  
494 Balearic front at 200 m depth. Oceanographic conditions in the NW Mediterranean Sea are mostly controlled  
495 by this current, which is associated with a permanent shelf/slope density front (Font et al., 1988; Salat, 1995)  
496 that plays a key role in the distribution of planktonic organisms (Sabatés et al., 2004). Our observations  
497 suggest that the strength of the Liguro-Provençal-Catalan current, associated here to the second mode of  
498 variability of the along-shore current (Fig. 7d), has increased from the mid-1990s to the early 2010s and  
499 reduced since (Fig. 9a, 9b). The weakened intensity of the current may be also associated to less export to  
500 the sea floor (Fig. 9b). Lévy et al. (2018) suggested that submesoscale ecological processes might play a  
501 significant role on productivity, affecting ocean biodiversity.



502  
503 Figure 9. Oceanographic processes from the surface to 400 m depth are represented under two contrasting scenarios. (a)  
504 Low temperature, strong front, and enhanced heat exchange associated with intense winter convection. High transport of  
505 organic matter and nutrients to the seafloor. High intensity of the Liguro-Provençal-Catalan current (Northern Current). (b)  
506 Increased temperature, weak front, and reduced heat exchange associated with weak winter convection. Limited transport  
507 of organic matter and nutrients to the seafloor. Reduced intensity of the Liguro-Provençal-Catalan current. The Levantine  
508 Intermediate Water (LIW) is also shown in both scenarios.



509           **4.4. Norway lobster catches track ocean dynamics changes over four decades**

510 Norway lobster LPUE and landings are well correlated between 2008 and 2024 (Fig. 3). While LPUE data are  
511 not available prior to 2008, Norway lobsters' landings have been used as a proxy for the status of the population  
512 since 1970. In order to explain the near-decadal fluctuations in Norway lobster landings we relate those  
513 observations to environmental variability patterns extracted with EOFs since 1986 (beginning of the  
514 environmental data availability period).

515

516 Norway lobster landings are marked by a slight decrease between the 1970s and early 1990s, followed by a  
517 rapid increase between the mid-1990s and the early-2010s and by another more pronounced decline since.  
518 Long-term analysis of landings of the Norway lobster shows a strong temporal correlation with temperature  
519 and salinity at 400 m depth. The widespread increase in temperature and salinity across the region is highly  
520 correlated to a decrease in landings of the Norway lobster. As stated before, the increase in temperature and  
521 salinity at 400 m depth, can be related with the reported warming and salinization trend of the LIW reported by  
522 (Margirier et al., 2020), which caused an increase of stratification and weakening of intermediate convection  
523 (Fig. 9b). This suggest that the reduction of deep convection may negatively affect Norway lobster's  
524 populations.

525

526 Our results support the fact that environmental conditions might be indirectly affecting the landings of the  
527 Norway lobster in the GSA 6 region. For example, González Herraiz et al. (2009) reported negative correlations  
528 between the North Atlantic Oscillation (NAO) and the LPUE of this species in the Porcupine bank (SW Ireland),  
529 linking stormy, warm and wet conditions with a loss of density of the Norway lobster and consequently LPUE  
530 low values. Furthermore, some studies have reported the impact of temperature and hydrographic factors in  
531 the larval phase of this species (Bailey et al., 1995; Dickey-Collas et al., 2000). It is known that abiotic factors  
532 such as temperature, salinity and circulation patterns have a direct effect on marine organisms' movement,  
533 migration and recruitment, or indirect by affecting the distribution and abundance of lower trophic levels (Nye  
534 et al., 2009). Then, could the reduction in Norway lobster landings and the observed deepening of its LPUE  
535 be attributed to a behavioral strategy to avoid higher temperatures? Might this downward shift result in reduced  
536 nutrient availability due to weaker vertical convection associated with increasing temperature and salinity at  
537 intermediate depths? Is the increase of stratification in intermediate waters retaining larvae and limiting their  
538 arrival to the sea floor? Additionally, are rising temperatures affecting lower trophic levels in ways that limit



539 food availability and, consequently, hinder the growth of Norway lobster populations? Our study suggests that  
540 the answers to those questions may be affirmative, but more studies need to be conducted.

541

#### 542 **4.5. Limitations of the study**

543 In this study, EOFs were performed on environmental data from reanalysis, not direct observations, assuming  
544 the variability inherent to these data are representative of the natural variability of the NW Mediterranean Sea.  
545 These reanalysis simulations, however, include data assimilation and have been validated and assessed  
546 through comparison to in-situ and satellite observations (Escudier et al., 2021). The low frequency variability,  
547 critical for this study, is also well resolved (Pinaridi et al., 2015). However, the EOF separation into statistical  
548 modes may also be imperfect.

549

550 Another limitation of this study is the use of landings pre-2008 as a proxy of biomass density. LPUE can be  
551 used as a proxy for the species abundance assuming that its trend follows the changes in the stock  
552 abundances (Hoyle et al., 2024; Leitão et al., 2022; Maunder & Punt, 2004; Mingote et al., 2024). Then, as  
553 landings and LPUE trends followed similar trends between 2008 and 2024 (Fig. 3), we assume this similarity  
554 extends to the whole time series and use landings because there is more available data and we want to  
555 evaluate the general trend and not a specific value.

556

#### 557 **4.6. Outlook and implications for fisheries management**

558 Climate projections indicate a global temperature increase of approximately 1.5 °C between 2030 and 2052  
559 (IPCC, 2018), which is expected to alter marine environmental conditions and affect species productivity.  
560 However, population dynamics are also influenced by natural environmental variability operating at multiple  
561 temporal scales. As a result, shifts in species composition may occur, with certain species potentially benefiting  
562 from changing conditions while others decline. Norway lobsters' trend in landings coincides with decadal-scale  
563 temperature variability, suggesting that environmental forcing plays an important role in shaping its population  
564 dynamics.

565

566 Disentangling fishing mortality from environmentally driven variability remains a major challenge, as both  
567 processes are intrinsically linked (Hilborn & Litzinger, 2009; Rothschild, 2007). Favorable environmental  
568 conditions may temporarily sustain fishing levels that would otherwise be unsustainable, whereas fishing



569 mortality can amplify the effects of adverse environmental conditions and accelerate stock declines (Cyr et al.,  
570 2025). Consequently, Norway lobster's stock that has historically been exploited sustainably may become  
571 overfished if its productivity decreases in response to unfavorable temperature regimes. This highlights the  
572 importance of incorporating environmental parameters, such as temperature variability, into stock assessment  
573 frameworks. Stock assessments are often primarily based on biological variables, and the inclusion of  
574 environmental variable may improve management advice and better reflect ecosystem dynamics.  
575 Understanding these natural fluctuations is therefore essential when evaluating fishing pressure. If a decline  
576 in abundance is driven by environmentally induced reductions in productivity, even reduced fishing effort may  
577 exert a disproportionate impact on an already weakened stock (Essington et al., 2015).

578

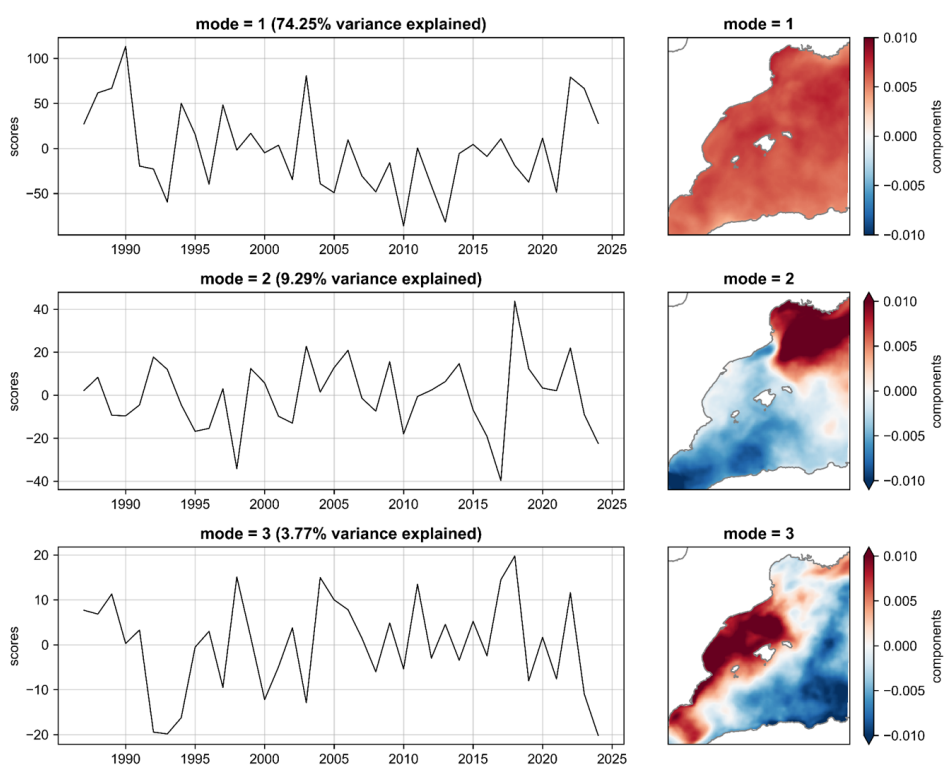
## 579 **5. Conclusions**

580 This study demonstrates that long-term fluctuations in Norway lobsters' landings in GSA 6 are driven by a  
581 combination of fishing pressure and, more importantly, environmental variability. Although fishing effort has  
582 steadily declined since 2004, this reduction alone cannot explain the sharp decline in landings and LPUE  
583 observed over the past 10–15 years. The results show that large-scale oceanographic changes in intermediate  
584 waters play a central role. The first EOF mode of temperature and salinity at 400 m, which explains nearly 78%  
585 of the variance, is strongly and negatively correlated with landings and LPUE, indicating that widespread  
586 warming and salinization at depth are associated with reduced catches. LPUE also shifted slightly deeper  
587 during years with positive temperature anomalies, suggesting behavioral responses to changing environmental  
588 conditions. Circulation patterns further contribute to the observed trends, with the strength of the  
589 Liguro-Provençal-Catalan Current and the North Balearic Front showing positive correlations with landings.  
590 Overall, the decline of the Norway lobster in recent years appears to be tied to intermediate-water warming,  
591 salinization, and changes in current intensity rather than to fishing effort alone. These findings highlight the  
592 need to incorporate environmental indicators into stock assessments and management strategies, particularly  
593 in the Mediterranean Sea, a recognized climate-change hotspot.

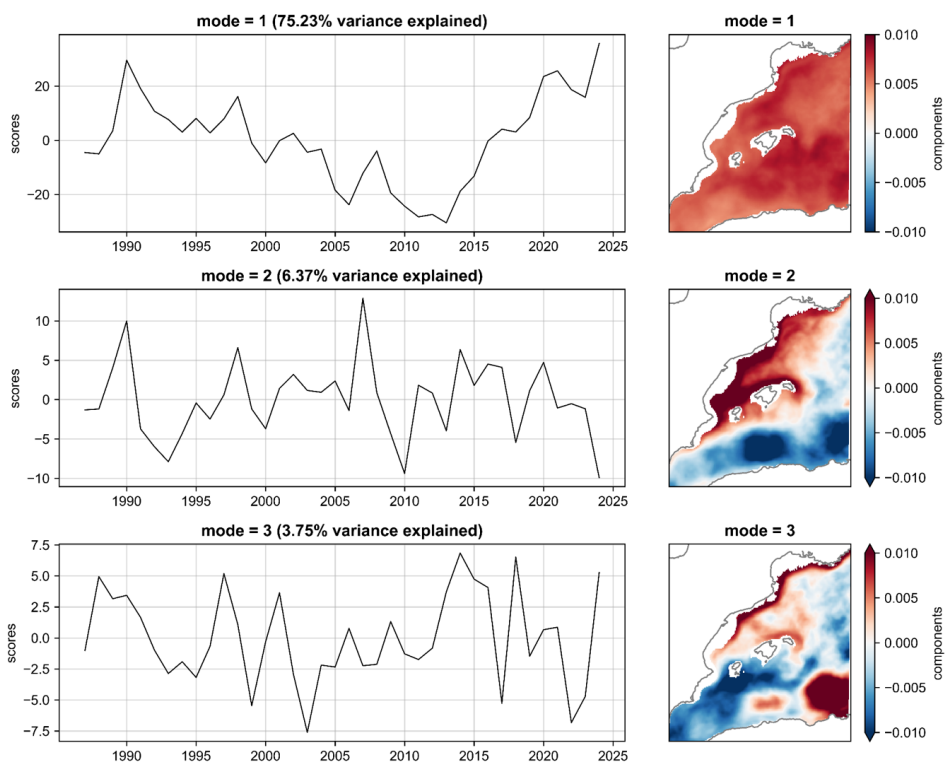


## 594 Appendices

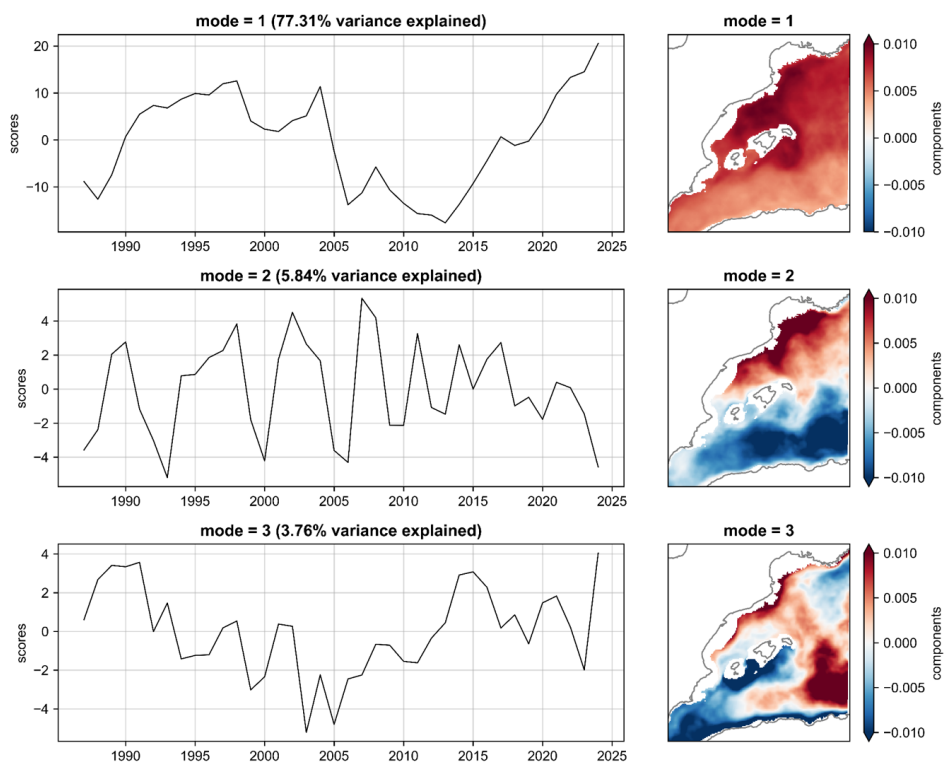
595 All figures from A1 to A15 show the EOF outputs for the environmental variables selected at discrete depths,  
596 as explained in Sect. 2.2. For all of them, the EOF components (spatial correlation maps) are shown on the  
597 right panels, with the scores (temporal variability of the components) on left panels. The percentage of the  
598 variance explained by each mode is also shown on top of the left panels.



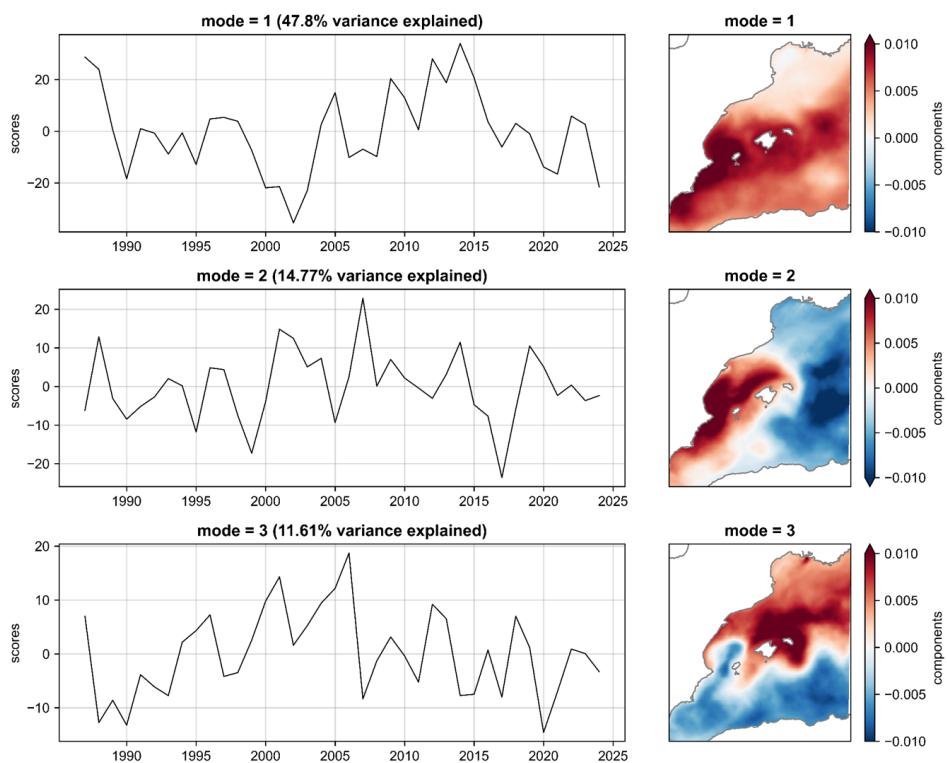
599 Figure A1. EOFs of the three first modes of variability for the de-trended annual temperature at surface between 1987 and  
600 2024. Here, positive score values indicate increasing temperature in areas where the spatial correlation is positive (red on  
601 the maps).



602 Figure A2. EOFs of the three first modes of variability for the de-trended annual temperature at 200 m between 1987 and  
603 2024. Here, positive score values indicate increasing temperature in areas where the spatial correlation is positive (red on  
604 the maps).

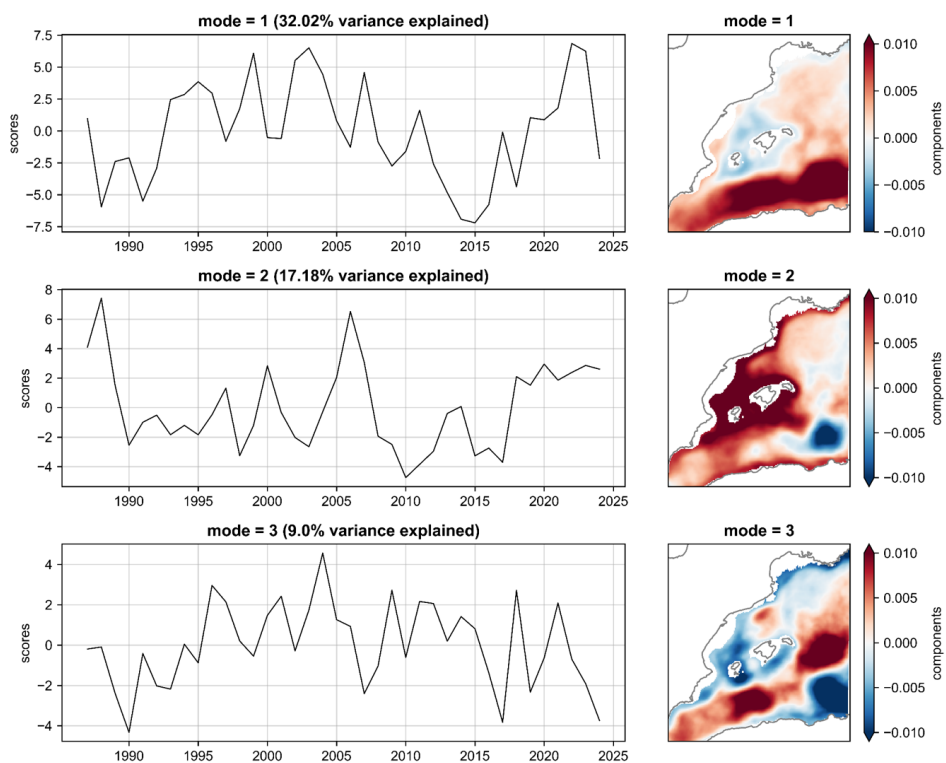


605 Figure A3. EOFs of the three first modes of variability for the de-trended annual temperature at 600 m between 1987 and  
606 2024. Here, positive score values indicate increasing temperature in areas where the spatial correlation is positive (red on  
607 the maps).



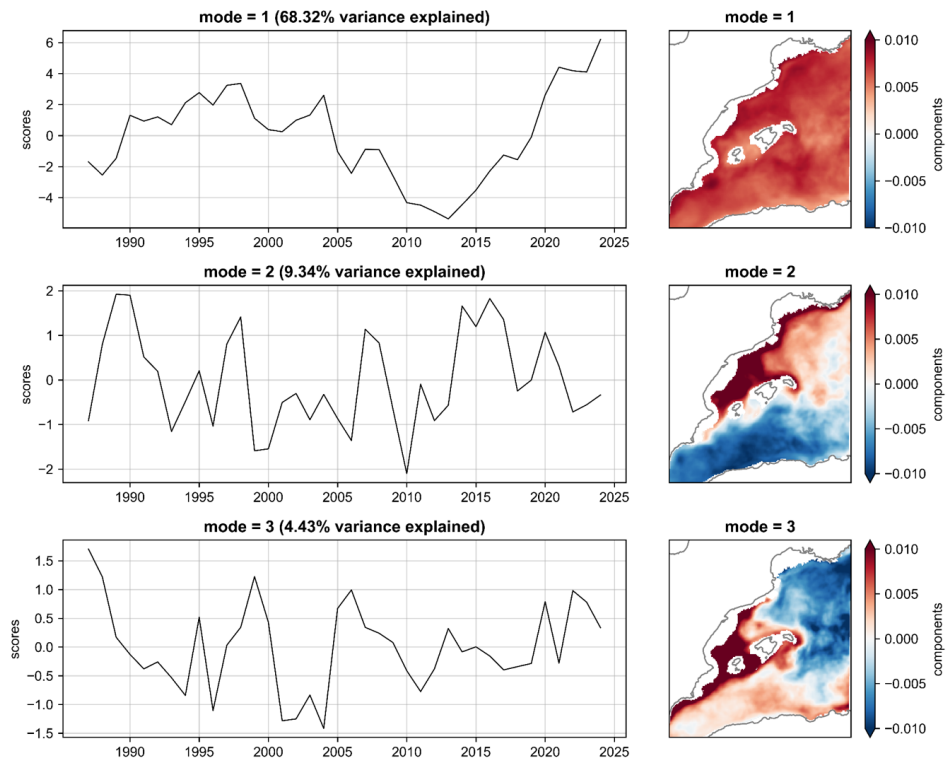
608 Figure A4. EOFs of the three first modes of variability for the de-trended annual salinity at surface between 1987 and 2024.

609 Here, positive score values indicate increasing salinity in areas where the spatial correlation is positive (red on the maps).



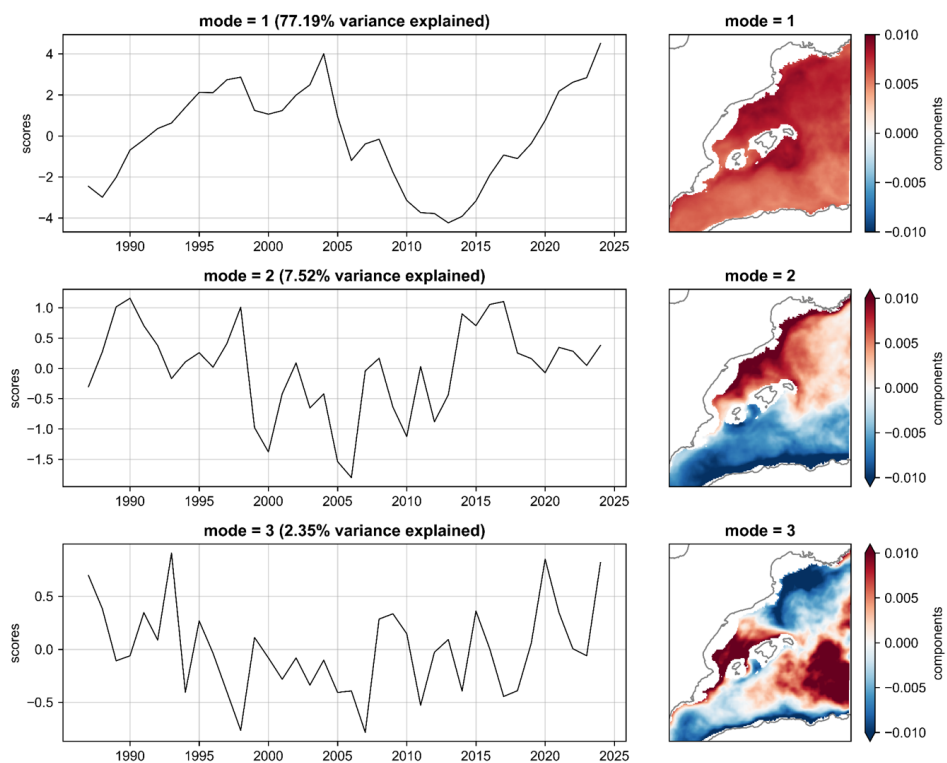
610 Figure A5. EOFs of the three first modes of variability for the de-trended annual salinity at 200 m between 1987 and 2024.

611 Here, positive score values indicate increasing salinity in areas where the spatial correlation is positive (red on the maps).



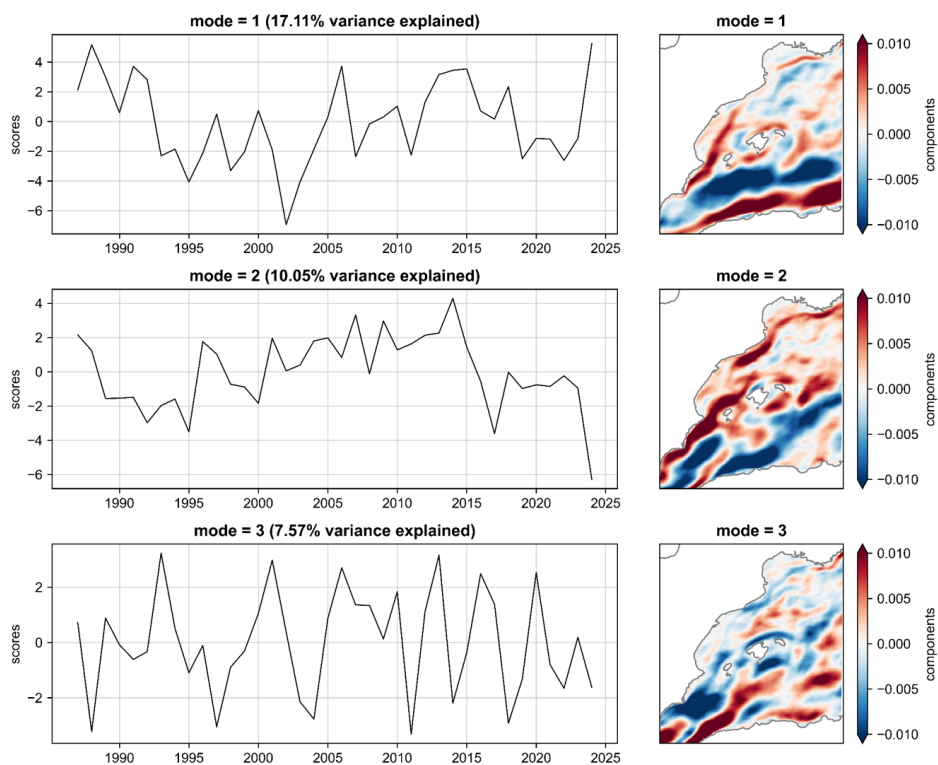
612 Figure A6. EOFs of the three first modes of variability for the de-trended annual salinity at 400 m between 1987 and 2024.

613 Here, positive score values indicate increasing salinity in areas where the spatial correlation is positive (red on the maps).

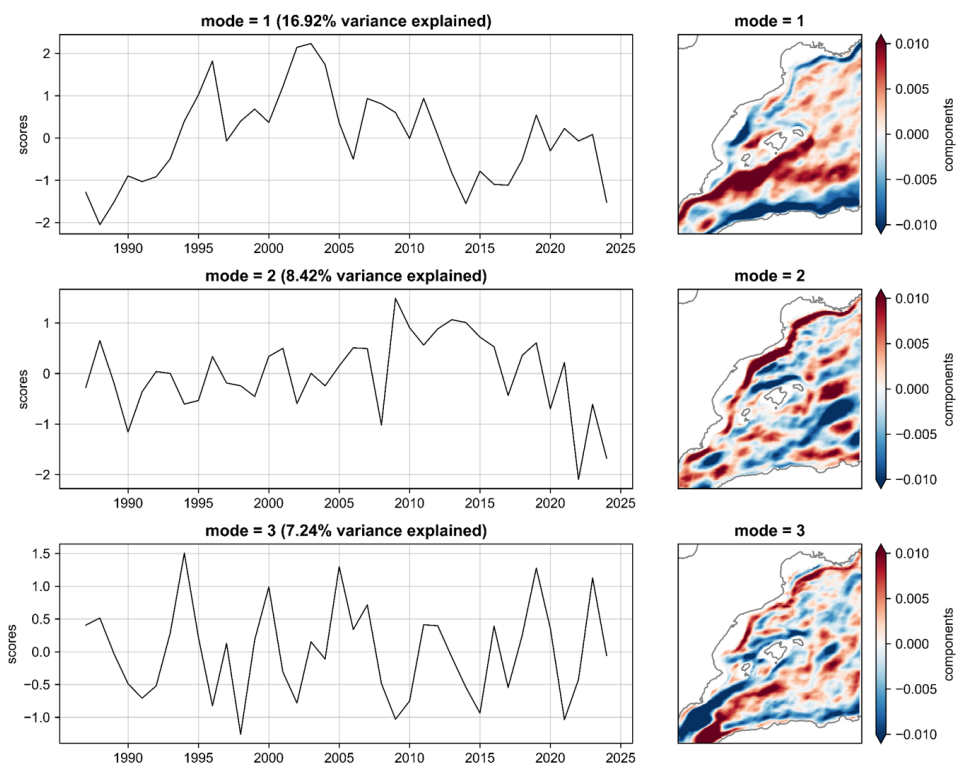


614 Figure A7. EOFs of the three first modes of variability for the de-trended annual salinity at 600 m between 1987 and 2024.

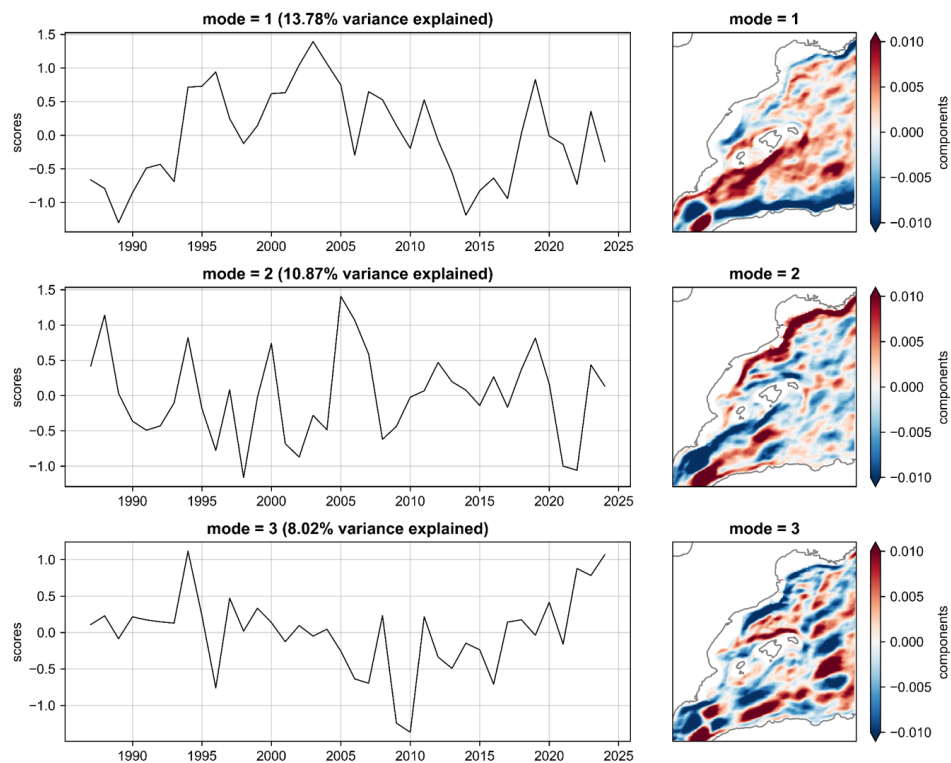
615 Here, positive score values indicate increasing salinity in areas where the spatial correlation is positive (red on the maps).



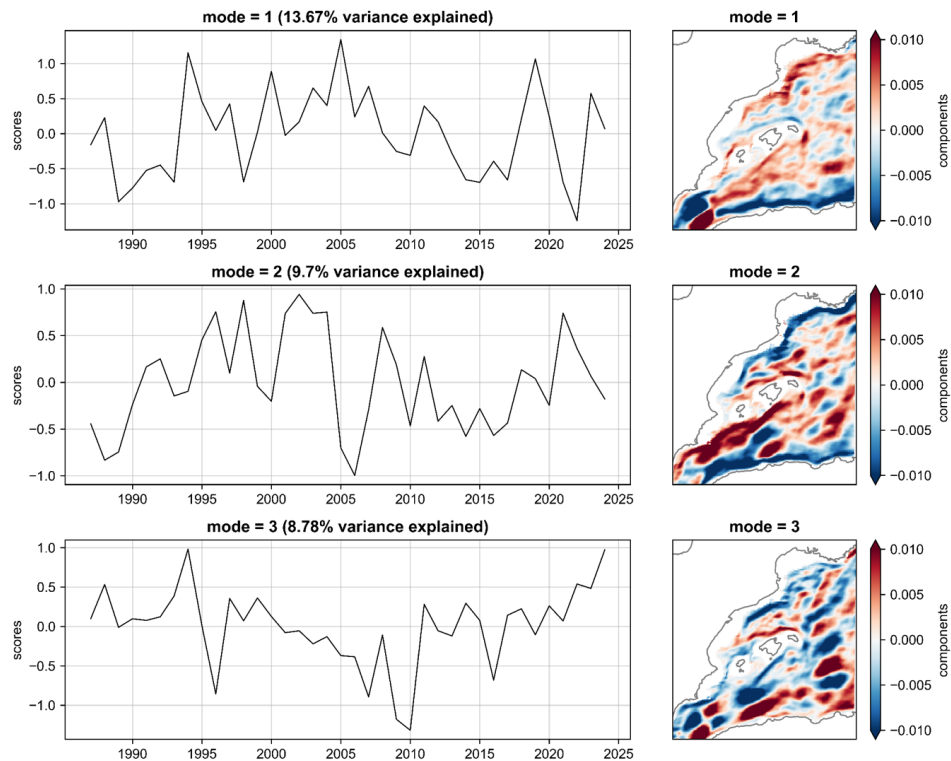
616 Figure A8. EOFs of the three first modes of variability for the de-trended annual current southwestward along shore (U) at  
617 surface between 1987 and 2024. Here, positive score values indicate increasing intensity of the current in areas where the  
618 spatial correlation is positive (red on the maps).



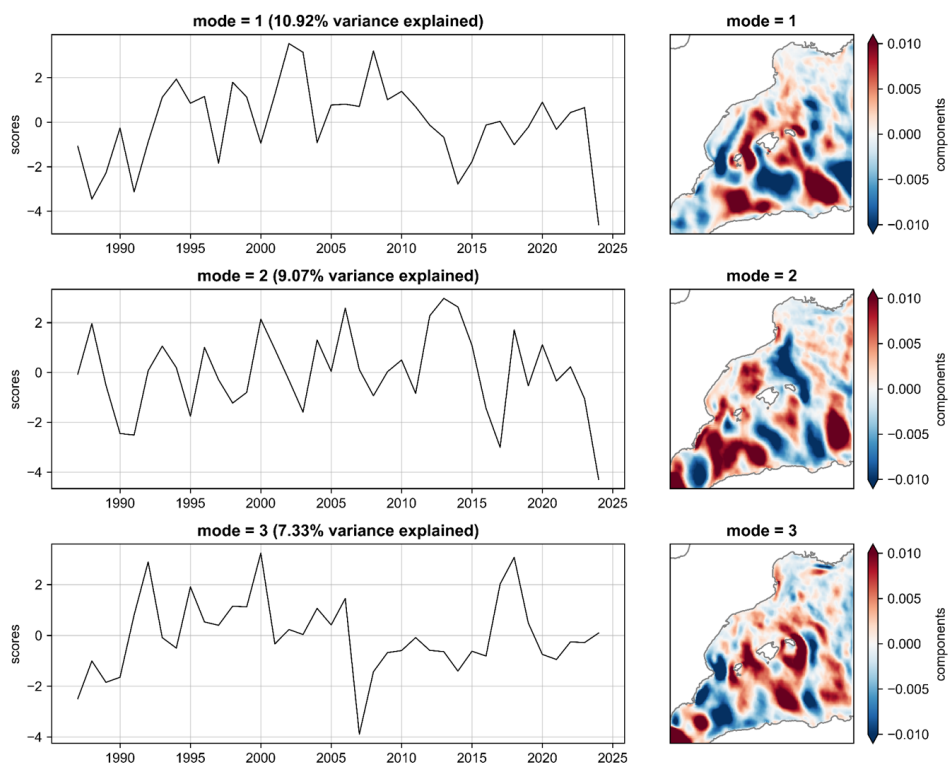
619 Figure A9. EOFs of the three first modes of variability for the de-trended annual current southwestward along shore (U) at  
620 200 m between 1987 and 2024. Here, positive score values indicate increasing intensity of the current in areas where the  
621 spatial correlation is positive (red on the maps).



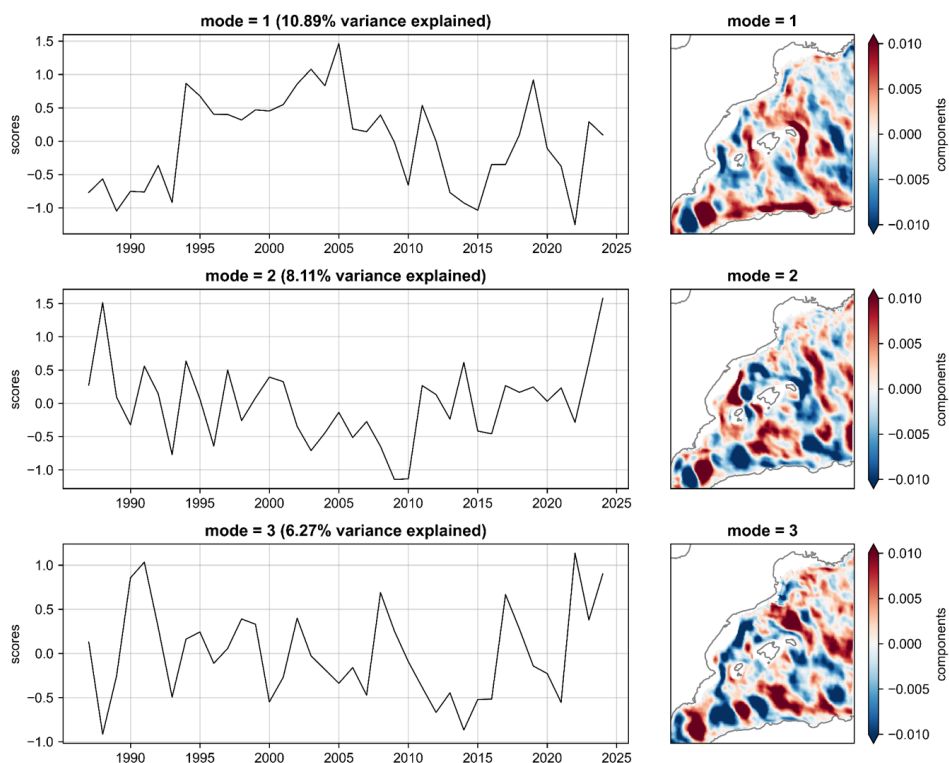
622 Figure A10. EOFs of the three first modes of variability for the de-trended annual current southwestward along shore (U)  
623 at 400 m between 1987 and 2024. Here, positive score values indicate increasing intensity of the current in areas where  
624 the spatial correlation is positive (red on the maps).



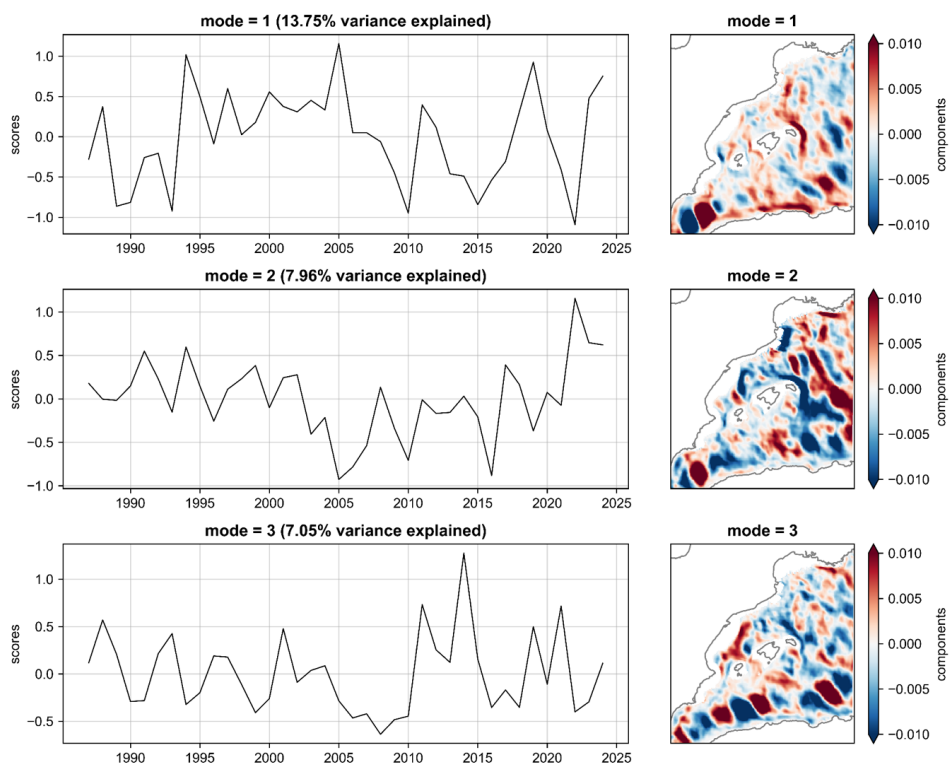
625 Figure A11. EOFs of the three first modes of variability for the de-trended annual current southwestward along shore (U)  
626 at 600 m between 1987 and 2024. Here, positive score values indicate increasing intensity of the current in areas where  
627 the spatial correlation is positive (red on the maps).



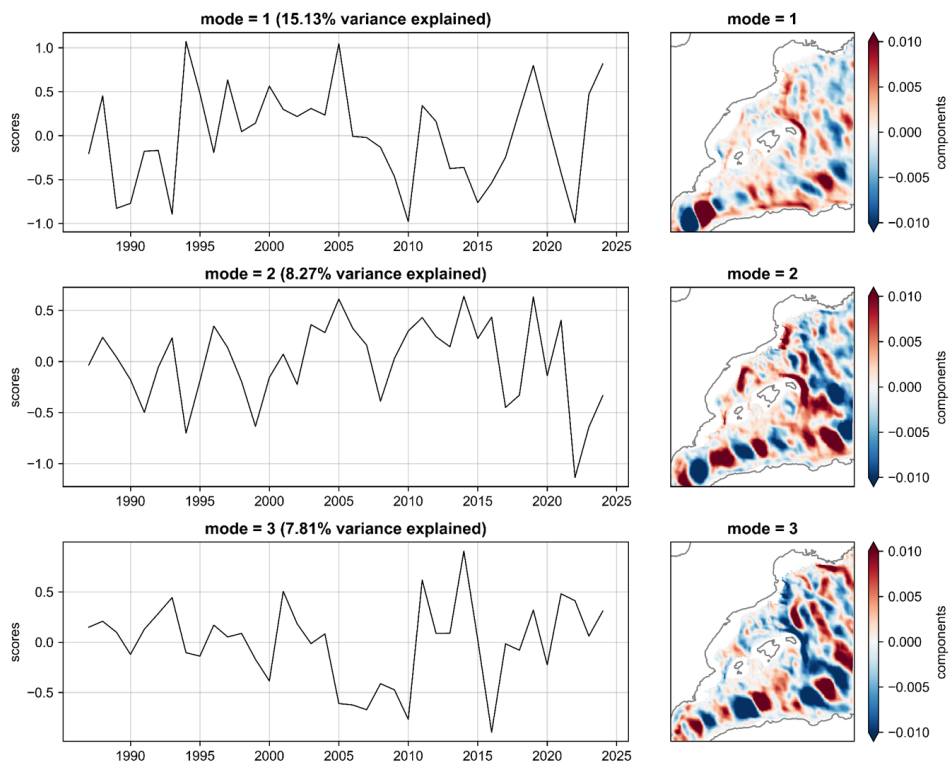
628 Figure A12. EOFs of the three first modes of variability for the de-trended annual current southeastward across shore (V)  
629 at surface between 1987 and 2024. Here, positive score values indicate increasing intensity of the current in areas where  
630 the spatial correlation is positive (red on the maps).



631 Figure A13. EOFs of the three first modes of variability for the de-trended annual current southeastward across shore (V)  
632 at 200 m between 1987 and 2024. Here, positive score values indicate increasing intensity of the current in areas where  
633 the spatial correlation is positive (red on the maps).



634 Figure A14. EOFs of the three first modes of variability for the de-trended annual current southeastward across shore (V)  
635 at 400 m between 1987 and 2024. Here, positive score values indicate increasing intensity of the current in areas where  
636 the spatial correlation is positive (red on the maps).



637 Figure A15. EOFs of the three first modes of variability for the de-trended annual current southeastward across shore (V)  
638 at 600 m between 1987 and 2024. Here, positive score values indicate increasing intensity of the current in areas where  
639 the spatial correlation is positive (red on the maps).



640 **Data availability statement**

641 Data and code used for this study are openly available in Zenodo at <https://doi.org/10.5281/zenodo.18874070>.

642 Environmental data were obtained from Marine Data Store of the E.U. Copernicus Marine Environment

643 Monitoring Service (CMEMS);

644 [https://doi.org/10.25423/CMCC/MEDSEA\\_MULTIYEAR\\_PHY\\_006\\_004\\_E3R1](https://doi.org/10.25423/CMCC/MEDSEA_MULTIYEAR_PHY_006_004_E3R1).

645

646 **Author contributions**

647 **Mireia G. Mingote**: conceptualization, methodology, data curation, visualization, formal analysis, writing

648 (original draft), writing (review and editing).

649 **Frédéric Cyr**: conceptualization, methodology, formal analysis, writing (original draft), writing (review and

650 editing), supervision.

651 **Eve Galimany**: conceptualization, writing (original draft), writing (review and editing), supervision.

652 **Ricardo Santos-Bethencourt**: data curation, visualization, writing (original draft), writing (review and editing).

653 **Jordi Isern-Fontanet**: conceptualization, writing (review and editing).

654 **Jordi Ribera-Altimir**: data curation, writing (review and editing).

655 **Joan Sala-Coromina**: data curation, writing (review and editing).

656 **Mariona Panisello-Garriga**: data curation, writing (review and editing).

657 **Joan B. Company**: conceptualization, writing (review and editing), supervision.

658

659 **Conflict of interest statement**

660 Authors declare no conflict of interest.

661

662 **Acknowledgements**

663 Thanks to all ICATMAR personnel and students who helped with the on-board data collection. Also, to all the

664 fishers that collaborate with this project.

665

666 **Funding**

667 This work was supported by the Catalan Research Institute for the Governance of the Sea (ICATMAR) and

668 financed by European Maritime and Fisheries Fund (EMFF) and the Catalan Directorate-General of Marine



669 Policy and Sustainable Fisheries by projects PESCAT (ARP029/18/00003), CGCAT (ARP140/20/000006) and  
670 SAP (BOE-A-2023-25106).

671

## 672 **References**

673 Abelló, P., Abella, Á., Adamidou, A., Jukic-Peladic, S., Maiorano, P., & Spedicato, M. T. (2002). Geographical  
674 patterns in abundance and population structure of *Nephrops norvegicus* and *Parapenaeus longirostris*  
675 (Crustacea: Decapoda) along the European Mediterranean coasts. *Scientia Marina*, 66(S2), Article  
676 S2. <https://doi.org/10.3989/scimar.2002.66s2125>

677 Adloff, F., Somot, S., Sevault, F., Jordà, G., Aznar, R., Déqué, M., Herrmann, M., Marcos, M., Dubois, C.,  
678 Padorno, E., Alvarez-Fanjul, E., & Gomis, D. (2015). Mediterranean Sea response to climate change  
679 in an ensemble of twenty first century scenarios. *Climate Dynamics*, 45(9), 2775-2802.  
680 <https://doi.org/10.1007/s00382-015-2507-3>

681 Aguzzi, J., Bahamon, N., & Marotta, L. (2009). The influence of light availability and predatory behavior of the  
682 decapod crustacean *Nephrops norvegicus* on the activity rhythms of continental margin prey  
683 decapods. *Marine Ecology*, 30(3), 366-375. <https://doi.org/10.1111/j.1439-0485.2008.00276.x>

684 Aguzzi, J., Sardà, F., Abelló, P., Company, J. B., & Rotllant, G. (2003). Diel and seasonal patterns of *Nephrops*  
685 *norvegicus* (Decapoda: Nephropidae) catchability in the western Mediterranean. *Marine Ecology*  
686 *Progress Series*, 258, 201-211. <https://doi.org/10.3354/meps258201>

687 Bahamon, N., Aguzzi, J., Ahumada-Sempol, M. Á., Bernardello, R., Reuschel, C., Company, J. B., Peters,  
688 F., Gordo, A., Navarro, J., Velásquez, Z., & Cruzado, A. (2020). Stepped Coastal Water Warming  
689 Revealed by Multiparametric Monitoring at NW Mediterranean Fixed Stations. *Sensors*, 20(9), 2658.  
690 <https://doi.org/10.3390/s20092658>

691 Bailey, N., Chapman, C. J., Afonso-Dias, M., & Turrell, W. (1995). The influence of hydrographic factors on  
692 *Nephrops* distribution and biology. *ICES CM*, 17, 13.

693 Balbín, R., López-Jurado, J. L., Flexas, M. M., Reglero, P., Vélez-Velchí, P., González-Pola, C., Rodríguez, J.  
694 M., García, A., & Alemany, F. (2014). Interannual variability of the early summer circulation around the  
695 Balearic Islands: Driving factors and potential effects on the marine ecosystem. *Journal of Marine*  
696 *Systems, The wrapping up of the IDEADOS project: International Workshop on Environment,*  
697 *Ecosystems and Demersal Resources, and Fisheries*, 138, 70-81.  
698 <https://doi.org/10.1016/j.jmarsys.2013.07.004>



- 699 Bilbao, R. A. F., Gregory, J. M., Bouttes, N., Palmer, M. D., & Stott, P. (2019). Attribution of ocean temperature  
700 change to anthropogenic and natural forcings using the temporal, vertical and geographical structure.  
701 *Climate Dynamics*, 53(9), 5389-5413. <https://doi.org/10.1007/s00382-019-04910-1>
- 702 Billett, D. S. M., Lampitt, R. S., Rice, A. L., & Mantoura, R. F. C. (1983). Seasonal sedimentation of  
703 phytoplankton to the deep-sea benthos. *Nature*, 302(5908), 520-522.  
704 <https://doi.org/10.1038/302520a0>
- 705 Cacho, I., Grimalt, J. O., & Canals, M. (2002). Response of the Western Mediterranean Sea to rapid climatic  
706 variability during the last 50,000 years: A molecular biomarker approach. *Journal of Marine Systems*,  
707 *MATER: MAss Transfer and Ecosystem Response*, 33-34, 253-272. [https://doi.org/10.1016/S0924-](https://doi.org/10.1016/S0924-7963(02)00061-1)  
708 [7963\(02\)00061-1](https://doi.org/10.1016/S0924-7963(02)00061-1)
- 709 Carreton, M., Galimany, E., Blanco, M., Garriga-Panisello, M., Colmenero, A. I., Balcells, M., Bustos, F.,  
710 Mingote, M. G., López-Pérez, C., Nos, D., Puigcerver-Segarra, X., Pujol-Baucells, M., Ramírez, J. G.,  
711 Ribera-Altimir, J., Rico, A. J., Rojas, A., Sala-Coromina, J., Santos-Bethencourt, R., Silvestre, M., ...  
712 Company, J. B. (2025). Understanding the spatio-temporal variability of fisheries data for better bottom  
713 trawling management practices in the Catalan margin (NW Mediterranean Sea). *Marine Policy*, 172,  
714 106512. <https://doi.org/10.1016/j.marpol.2024.106512>
- 715 Castellón, A., Font, J., & García-Ladona, E. (1990). The Liguro-Provençal-Catalan current (NW Mediterranean)  
716 observed by Doppler profiling in the Balearic Sea. *Scientia Marina*, 54(3), 269-276.
- 717 Chapman, C., & Howard, F. (1988). *Environmental influences on Norway lobster (Nephrops norvegicus)*  
718 *populations and their implications for fishery management*. 59, 343-353.
- 719 Chen, I.-C., Hill, J. K., Ohlemüller, R., Roy, D. B., & Thomas, C. D. (2011). Rapid Range Shifts of Species  
720 Associated with High Levels of Climate Warming. *Science*, 333(6045), 1024-1026.  
721 <https://doi.org/10.1126/science.1206432>
- 722 Chust, G., Villarino, E., McLean, M., Mieszkowska, N., Benedetti-Cecchi, L., Bulleri, F., Ravaglioli, C., Borja,  
723 A., Muxika, I., Fernandes-Salvador, J. A., Ibaibarriaga, L., Uriarte, A., Revilla, M., Villate, F., Iriarte, A.,  
724 Uriarte, I., Zervoudaki, S., Carstensen, J., Somerfield, P. J., ... Lindegren, M. (2024). Cross-basin and  
725 cross-taxa patterns of marine community tropicalization and deborealization in warming European  
726 seas. *Nature Communications*, 15(1), 2126. <https://doi.org/10.1038/s41467-024-46526-y>
- 727 Company, J. B., Puig, P., Sardà, F., Palanques, A., Latasa, M., & Scharek, R. (2008). Climate Influence on  
728 Deep Sea Populations. *PLOS ONE*, 3(1), e1431. <https://doi.org/10.1371/journal.pone.0001431>



- 729 Cyr, F., Adamack, A. T., Bélanger, D., Koen-Alonso, M., Mullaney, D., Murphy, H., Regular, P., & Pepin, P.  
730 (2025). Environmental control on the productivity of a heavily fished ecosystem. *Nature*  
731 *Communications*, 16(1), 5277. <https://doi.org/10.1038/s41467-025-60453-6>
- 732 Dickey-Collas, M., McQuaid, N., Armstrong, M. J., Allen, M., & Briggs, R. P. (2000). Temperature-dependent  
733 stage durations of Irish Sea *Nephrops* larvae. *Journal of Plankton Research*, 22(4), 749-760.  
734 <https://doi.org/10.1093/plankt/22.4.749>
- 735 Durrieu de Madron, X., Guieu, C., Sempéré, R., Conan, P., Cossa, D., D'Ortenzio, F., Estoumel, C., Gazeau,  
736 F., Rabouille, C., Stemmann, L., Bonnet, S., Diaz, F., Koubbi, P., Radakovitch, O., Babin, M., Baklouti,  
737 M., Bancon-Montigny, C., Belviso, S., Bensoussan, N., ... Verney, R. (2011). Marine ecosystems'  
738 responses to climatic and anthropogenic forcings in the Mediterranean. *Progress in Oceanography*,  
739 91(2), 97-166. <https://doi.org/10.1016/j.pocean.2011.02.003>
- 740 Escudier, R., Clementi, E., Cipollone, A., Pistoia, J., Drudi, M., Grandi, A., Lyubartsev, V., Lecci, R., Aydogdu,  
741 A., Delrosso, D., Omar, M., Masina, S., Coppini, G., & Pinardi, N. (2021). A High Resolution Reanalysis  
742 for the Mediterranean Sea. *Frontiers in Earth Science*, 9. <https://doi.org/10.3389/feart.2021.702285>
- 743 Escudier, R., Clementi, E., Omar, M., Cipollone, A., Pistoia, J., Aydogdu, A., Drudi, M., Grandi, A., Lyubartsev,  
744 V., Lecci, R., Cretí, S., Masina, S., Coppini, G., & Pinardi, N. (2020). *Mediterranean Sea Physical*  
745 *Reanalysis (CMEMS MED-Currents) (Version 1)* [Dataset]. Copernicus Monitoring Environment  
746 Marine Service (CMEMS).  
747 [https://doi.org/https://doi.org/10.25423/CMCC/MEDSEA\\_MULTIYEAR\\_PHY\\_006\\_004\\_E3R1](https://doi.org/https://doi.org/10.25423/CMCC/MEDSEA_MULTIYEAR_PHY_006_004_E3R1)
- 748 Essington, T., Moriarty, P., Froehlich, H., Hodgson, E., Koehn, L., Oken, K., Siple, M., & Stawitz, C. (2015).  
749 Fishing amplifies forage fish population collapses. *Proceedings of the National Academy of Sciences*  
750 *of the United States of America*, 112. <https://doi.org/10.1073/pnas.1422020112>
- 751 FAO. (2025). *Nephrops norvegicus* Linnaeus, 1758 [Fisheries and Aquaculture].  
752 <https://www.fao.org/fishery/en/aqspecies/2647/en>
- 753 Fariña, A. C., & González Herraiz, I. (2003). Trends in catch-per-unit-effort, stock biomass and recruitment in  
754 the North and Northwest Iberian Atlantic *Nephrops* stocks. *Fisheries Research*.
- 755 Font, J., Salat, J., & Tintore, J. (1988). Permanent features of the circulation in the Catalan Sea. *Oceanologica*  
756 *Acta, Special Issue*. Oceanographie Pelagique Mediterraneene, Villefranche-sur-Mer (France), 16-20  
757 Sep 1988. <https://archimer.ifremer.fr/doc/00267/37808/>



- 758 Gage, J. D. (2002). Food Inputs, utilisation, carbon flow and energetics. En P. Tyler (Ed.), *Ecosystems of the*  
759 *world* (pp. 313-380). Elsevier Science, Amsterdam.
- 760 GEBCO Compilation Group. (2024). *GEBCO 2024 Grid* [Dataset]. [https://doi.org/doi:10.5285/1c44ce99-0a0d-](https://doi.org/doi:10.5285/1c44ce99-0a0d-5f4f-%20e063-7086abc0ea0f)  
761 [5f4f-%20e063-7086abc0ea0f](https://doi.org/doi:10.5285/1c44ce99-0a0d-5f4f-%20e063-7086abc0ea0f)
- 762 Giorgi, F. (2006). Climate change hot-spots. *Geophysical Research Letters*, 33(8).  
763 <https://doi.org/10.1029/2006GL025734>
- 764 González Herraiz, I., Fariña, A. C., Freire, J., & Cancelo de la Torre, J. R. (2015). Exploring long-term variability  
765 of *Nephrops norvegicus* landing per unit effort (LPUE) off North Galicia (NW Spain). *Fisheries*  
766 *Research*, 165, 121-126. <https://doi.org/10.1016/j.fishres.2014.12.020>
- 767 González Herraiz, I., Torres, M. A., Fariña, A. C., Freire, J., & Cancelo, J. R. (2009). The NAO index and the  
768 long-term variability of *Nephrops norvegicus* population and fishery off West of Ireland. *Fisheries*  
769 *Research*, 98(1), 1-7. <https://doi.org/10.1016/j.fishres.2009.03.006>
- 770 Hannachi, A., Jolliffe, I. T., & Stephenson, D. B. (2007). Empirical orthogonal functions and related techniques  
771 in atmospheric science: A review. *International Journal of Climatology*, 27(9), 1119-1152.  
772 <https://doi.org/10.1002/joc.1499>
- 773 Hilborn, R., & Litzinger, E. (2009). Causes of Decline and Potential for Recovery of Atlantic Cod Populations.  
774 *The Open Fish Science Journal*, 2. <https://doi.org/10.2174/1874401X00902010032>
- 775 Hoyle, S. D., Campbell, R. A., Ducharme-Barth, N. D., Grüss, A., Moore, B. R., Thorson, J. T., Tremblay-  
776 Boyer, L., Winker, H., Zhou, S., & Maunder, M. N. (2024). Catch per unit effort modelling for stock  
777 assessment: A summary of good practices. *Fisheries Research*, 269, 106860.  
778 <https://doi.org/10.1016/j.fishres.2023.106860>
- 779 ICATMAR. (2025). *Economic Trends in Landings of the Fishing Sector in Catalonia 2024 (ICATMAR, 25-04)*  
780 (p. 209). Institut Català de Recerca per a la Governança del Mar (ICATMAR).  
781 <https://doi.org/10.20350/digitalCSIC/17287>
- 782 IPCC. (2018). *Global Warming of 1.5°C: IPCC Special Report on Impacts of Global Warming of 1.5°C above*  
783 *Pre-industrial Levels in Context of Strengthening Response to Climate Change, Sustainable*  
784 *Development, and Efforts to Eradicate Poverty* (1.<sup>a</sup> ed.). Cambridge University Press.  
785 <https://doi.org/10.1017/9781009157940>



- 786 Johnson, M. P., Lordan, C., & Power, A. M. (2013). Habitat and Ecology of *Nephrops norvegicus*. En M. L.  
787 Johnson & M. P. Johnson (Eds.), *Advances in Marine Biology* (Vol. 64, pp. 27-63). Academic Press.  
788 <https://doi.org/10.1016/B978-0-12-410466-2.00002-9>
- 789 Jorda, G., Marbà, N., Bennett, S., Santana-Garcon, J., Agusti, S., & Duarte, C. M. (2020). Ocean warming  
790 compresses the three-dimensional habitat of marine life. *Nature Ecology & Evolution*, 4(1), 109-114.  
791 <https://doi.org/10.1038/s41559-019-1058-0>
- 792 Leitão, P., Sousa, L., Castro, M., & Campos, A. (2022). Time and spatial trends in landing per unit of effort as  
793 support to fisheries management in a multi-gear coastal fishery. *PLOS ONE*, 17(7), e0258630.  
794 <https://doi.org/10.1371/journal.pone.0258630>
- 795 Lévy, M., Franks, P. J. S., & Smith, K. S. (2018). The role of submesoscale currents in structuring marine  
796 ecosystems. *Nature Communications*, 9(1), 4758. <https://doi.org/10.1038/s41467-018-07059-3>
- 797 MAPA. (2025). *Informe anual de la actividad de la flota pesquera española 2025 (datos 2023)*. Ministerio de  
798 Agricultura, Pesca y Alimentación, Secretaría General de Pesca.  
799 [https://www.mapa.gob.es/dam/mapa/contenido/pesca/temas--nuevo/registro-de-flota--flota-  
pesquera-espanola/registro-general-de-la-flota-pesquera/informes-anuales-de-la-flota-pesquera.-  
planes-de-accion/informe-anual-flota-2025.pdf](https://www.mapa.gob.es/dam/mapa/contenido/pesca/temas--nuevo/registro-de-flota--flota-<br/>800 pesquera-espanola/registro-general-de-la-flota-pesquera/informes-anuales-de-la-flota-pesquera.-<br/>801 planes-de-accion/informe-anual-flota-2025.pdf)
- 802 Margirier, F., Testor, P., Heslop, E., Mallil, K., Bosse, A., Houpert, L., Mortier, L., Bouin, M.-N., Coppola, L.,  
803 D'Ortenzio, F., Durrieu de Madron, X., Mourre, B., Prieur, L., Raimbault, P., & Taillandier, V. (2020).  
804 Abrupt warming and salinification of intermediate waters interplays with decline of deep convection in  
805 the Northwestern Mediterranean Sea. *Scientific Reports*, 10(1), 20923.  
806 <https://doi.org/10.1038/s41598-020-77859-5>
- 807 Martín, P. (1991). *La pesca en Cataluña y Valencia (NO Mediterráneo): Análisis de las series históricas de*  
808 *captura y esfuerzo*. Instituto de Ciencias del Mar.
- 809 Maunder, M. N., & Punt, A. E. (2004). Standardizing catch and effort data: A review of recent approaches.  
810 *Fisheries Research, Models in Fisheries Research: GLMs, GAMS and GLMMs*, 70(2), 141-159.  
811 <https://doi.org/10.1016/j.fishres.2004.08.002>
- 812 Maynou, F., & Sardà, F. (1997). *Nephrops norvegicus* population and morphometrical characteristics in relation  
813 to substrate heterogeneity. *Fisheries Research*, 30(1), 139-149. [https://doi.org/10.1016/S0165-  
7836\(96\)00549-8](https://doi.org/10.1016/S0165-<br/>814 7836(96)00549-8)



- 815 Maynou, F., & Sardà, F. (2001). Influence of environmental factors on commercial trawl catches of *Nephrops*  
816 *norvegicus* (L.). *ICES Journal of Marine Science*, 58(6), 1318-1325.  
817 <https://doi.org/10.1006/jmsc.2001.1091>
- 818 McLean, M., Mouillot, D., Maureaud, A. A., Hattab, T., MacNeil, M. A., Goberville, E., Lindegren, M., Engelhard,  
819 G., Pinsky, M., & Auber, A. (2021). Disentangling tropicalization and deborealization in marine  
820 ecosystems under climate change. *Current Biology*, 31(21), 4817-4823.e5.  
821 <https://doi.org/10.1016/j.cub.2021.08.034>
- 822 Millot, C., & Taupier-Letage, I. (2005). Circulation in the Mediterranean Sea. En A. Saliot (Ed.), *The*  
823 *Mediterranean Sea* (pp. 29-66). Springer. <https://doi.org/10.1007/b107143>
- 824 Mingote, M. G., Galimany, E., Sala-Coromina, J., Bahamon, N., Ribera-Altimir, J., Santos-Bethencourt, R.,  
825 Clavel-Henry, M., & Company, J. B. (2024). Warming and salinization effects on the deep-water rose  
826 shrimp, *Parapenaeus longirostris*, distribution along the NW Mediterranean Sea: Implications for  
827 bottom trawl fisheries. *Marine Pollution Bulletin*, 198, 115838.  
828 <https://doi.org/10.1016/j.marpolbul.2023.115838>
- 829 Munn, T. (Ed.). (2002). *Encyclopedia of global environmental change*. Wiley.
- 830 Newland, P. L., Neil, D. M., & Chapman, C. J. (1988). The reactions of the Norway lobster, *Nephrops*  
831 *norvegicus* (L.), to water currents. *Marine Behaviour and Physiology*, 13(3), 301-313.  
832 <https://doi.org/10.1080/10236248809378680>
- 833 Nigam, T., Escudier, R., Pistoia, J., Aydogdu, A., Omar, M., Clementi, E., Cipollone, A., Drudi, M., Grandi, A.,  
834 Mariani, A., Lyubartsev, V., Lecci, R., Cretí, S., Masina, S., Coppini, G., & Pinardi, N. (2021).  
835 *Mediterranean Sea Physical Reanalysis INTERIM (CMEMS MED-Currents, E3R1i system) (Version*  
836 *1) [Dataset]*. Copernicus Monitoring Environment Marine Service (CMEMS).  
837 [https://doi.org/https://doi.org/10.25423/CMCC/MEDSEA\\_MULTIYEAR\\_PHY\\_006\\_004\\_E3R1I](https://doi.org/https://doi.org/10.25423/CMCC/MEDSEA_MULTIYEAR_PHY_006_004_E3R1I)
- 838 NOAA, N. (2024). Monthly global climate report for annual 2023. URL: <https://www.ncei.noaa.gov/access/monitoring/monthly-report/global/202313>.
- 840 Nye, J. A., Link, J. S., Hare, J. A., & Overholtz, W. J. (2009). Changing spatial distribution of fish stocks in  
841 relation to climate and population size on the Northeast United States continental shelf. *Marine*  
842 *Ecology Progress Series*, 393, 111-129. <https://doi.org/10.3354/meps08220>
- 843 Parmesan, C., & Yohe, G. (2003). A globally coherent fingerprint of climate change impacts across natural  
844 systems. *Nature*, 421(6918), 37-42. <https://doi.org/10.1038/nature01286>



- 845 Pastor, F., Valiente, J. A., & Khodayar, S. (2020). A Warming Mediterranean: 38 Years of Increasing Sea  
846 Surface Temperature. *Remote Sensing*, 12(17), Article 17. <https://doi.org/10.3390/rs12172687>
- 847 Pecl, G. T., Araújo, M. B., Bell, J. D., Blanchard, J., Bonebrake, T. C., Chen, I.-C., Clark, T. D., Colwell, R. K.,  
848 Danielsen, F., Evengård, B., Falconi, L., Ferrier, S., Frusher, S., Garcia, R. A., Griffis, R. B., Hobday,  
849 A. J., Janion-Scheepers, C., Jarzyna, M. A., Jennings, S., ... Williams, S. E. (2017). Biodiversity  
850 redistribution under climate change: Impacts on ecosystems and human well-being. *Science*,  
851 355(6332), eaai9214. <https://doi.org/10.1126/science.aai9214>
- 852 Perry, A. L., Low, P. J., Ellis, J. R., & Reynolds, J. D. (2005). Climate Change and Distribution Shifts in Marine  
853 Fishes. *Science*, 308(5730), 1912-1915. <https://doi.org/10.1126/science.1111322>
- 854 Pinardi, N., Zavatarelli, M., Adani, M., Coppini, G., Fratianni, C., Oddo, P., Simoncelli, S., Tonani, M.,  
855 Lyubartsev, V., Dobricic, S., & Bonaduce, A. (2015). Mediterranean Sea large-scale low-frequency  
856 ocean variability and water mass formation rates from 1987 to 2007: A retrospective analysis. *Progress  
857 in Oceanography, Oceanography of the Arctic and North Atlantic Basins*, 132, 318-332.  
858 <https://doi.org/10.1016/j.pocean.2013.11.003>
- 859 Pinsky, M. L., Fenichel, E., Fogarty, M., Levin, S., McCay, B., St. Martin, K., Selden, R. L., & Young, T. (2021).  
860 Fish and fisheries in hot water: What is happening and how do we adapt? *Population Ecology*, 63(1),  
861 17-26. <https://doi.org/10.1002/1438-390X.12050>
- 862 Pinsky, M. L., Selden, R. L., & Kitchel, Z. J. (2020). Climate-Driven Shifts in Marine Species Ranges: Scaling  
863 from Organisms to Communities. *Annual Review of Marine Science*, 12(Volume 12, 2020), 153-179.  
864 <https://doi.org/10.1146/annurev-marine-010419-010916>
- 865 Pisano, A., Marullo, S., Artale, V., Falcini, F., Yang, C., Leonelli, F. E., Santoleri, R., & Buongiorno Nardelli, B.  
866 (2020). New Evidence of Mediterranean Climate Change and Variability from Sea Surface  
867 Temperature Observations. *Remote Sensing*, 12(1), Article 1. <https://doi.org/10.3390/rs12010132>
- 868 Poloczanska, E. S., Brown, C. J., Sydeman, W. J., Kiessling, W., Schoeman, D. S., Moore, P. J., Brander, K.,  
869 Bruno, J. F., Buckley, L. B., Burrows, M. T., Duarte, C. M., Halpern, B. S., Holding, J., Kappel, C. V.,  
870 O'Connor, M. I., Pandolfi, J. M., Parmesan, C., Schwing, F., Thompson, S. A., & Richardson, A. J.  
871 (2013). Global imprint of climate change on marine life. *Nature Climate Change*, 3(10), 919-925.  
872 <https://doi.org/10.1038/nclimate1958>
- 873 Puig, P., Madron, X. D. de, Salat, J., Schroeder, K., Martín, J., Karageorgis, A. P., Palanques, A., Roullier, F.,  
874 Lopez-Jurado, J. L., Emelianov, M., Moutin, T., & Houpert, L. (2013). Thick bottom nepheloid layers



875 in the western Mediterranean generated by deep dense shelf water cascading. *Progress in*  
876 *Oceanography*, 111, 1-23. <https://doi.org/10.1016/j.pocean.2012.10.003>

877 Punzón, A., Rueda, L., Rodríguez-Basalo, A., Hidalgo, M., Oliver, P., Castro, J., Gil, J., Esteban, A., Gil de  
878 Sola, L., & Massutí, E. (2020). History of the Spanish demersal fishery in the Atlantic and  
879 Mediterranean Seas. *ICES Journal of Marine Science*, 77(2), 553-566.  
880 <https://doi.org/10.1093/icesjms/fsz231>

881 Rhein, M., Rintoul, S., Aoki, S., Campos, E., Chambers, D., Feely, R., & Wang, F. (2013). Observations:  
882 Ocean. In: *Climate Change 2013: The Physical Science Basis. Contribution of Working Group I to the*  
883 *Fifth Assessment Report of the Intergovernmental Panel on Climate Change. Fifth Assessment Report*  
884 *of the Intergovernmental Panel on Climate Change*, 255-315.

885 Ribera-Altimir, J., Llorach-Tó, G., Sala-Coromina, J., Company, J. B., & Galimany, E. (2023). Fisheries data  
886 management systems in the NW Mediterranean: From data collection to web visualization. *Database*,  
887 2023, baad067. <https://doi.org/10.1093/database/baad067>

888 Rieger, N., & Levang, S. J. (2024). xeofs: Comprehensive EOF analysis in Python with xarray. *Journal of Open*  
889 *Source Software*, 9(93), 6060. <https://doi.org/10.21105/joss.06060>

890 Rothschild, B. J. (2007). Coherence of Atlantic Cod Stock Dynamics in the Northwest Atlantic Ocean.  
891 *Transactions of the American Fisheries Society*, 136(3), 858-874. <https://doi.org/10.1577/T06-213.1>

892 Sabatés, A., Salat, J., & Masó, M. (2004). Spatial heterogeneity of fish larvae across a meandering current in  
893 the northwestern Mediterranean. *Deep Sea Research Part I: Oceanographic Research Papers*, 51(4),  
894 545-557. <https://doi.org/10.1016/j.dsr.2003.11.003>

895 Sala-Coromina, J., García, J. A., Martín, P., Fernandez-Arcaya, U., & Recasens, L. (2021). European hake  
896 (*Merluccius merluccius*, Linnaeus 1758) spillover analysis using VMS and landings data in a no-take  
897 zone in the northern Catalan coast (NW Mediterranean). *Fisheries Research*, 237, 105870.  
898 <https://doi.org/10.1016/j.fishres.2020.105870>

899 Salat, J. (1995). *The interaction between the Catalan and Balearic currents in the southern Catalan Sea*.  
900 <https://digital.csic.es/handle/10261/194237>

901 Sardá, F. (1995). *A review (1967-1990) of some aspects of the life history of Nephrops norvegicus* [Report].  
902 ICES MSS Vol.199 - Shellfish life histories and shellfishery models.  
903 <https://doi.org/10.17895/ices.pub.19271384.v1>



- 904 Sardà, F. (1998). *Nephrops norvegicus* (L.): Comparative biology and fishery in the Mediterranean Sea.  
905 Introduction, conclusions and recommendations. *Scientia Marina*, 62(S1), Article S1.  
906 <https://doi.org/10.3989/scimar.1998.62s15>
- 907 Schroeder, K., Chiggiato, J., Josey, S. A., Borghini, M., Aracri, S., & Sparnocchia, S. (2017). Rapid response  
908 to climate change in a marginal sea. *Scientific Reports*, 7(1), 4065. [https://doi.org/10.1038/s41598-](https://doi.org/10.1038/s41598-017-04455-5)  
909 017-04455-5
- 910 Tuck, I. D., Chapman, C. J., & Atkinson, R. J. A. (1997). Population biology of the Norway lobster, *Nephrops*  
911 *norvegicus* (L.) in the Firth of Clyde, Scotland – I: Growth and density. *ICES Journal of Marine Science*,  
912 54(1), 125-135. <https://doi.org/10.1006/jmsc.1996.0179>
- 913 Tully, O., & Hillis, J. P. (1995). Causes and spatial scales of variability in population structure of *Nephrops*  
914 *norvegicus* (L.) in the Irish Sea. *Fisheries Research*, 2.
- 915 Vergés, A., Steinberg, P. D., Hay, M. E., Poore, A. G. B., Campbell, A. H., Ballesteros, E., Heck, K. L., Booth,  
916 D. J., Coleman, M. A., Feary, D. A., Figueira, W., Langlois, T., Marzinelli, E. M., Mizerek, T., Mumby,  
917 P. J., Nakamura, Y., Roughan, M., van Sebille, E., Gupta, A. S., ... Wilson, S. K. (2014). The  
918 tropicalization of temperate marine ecosystems: Climate-mediated changes in herbivory and  
919 community phase shifts. *Proceedings of the Royal Society B: Biological Sciences*, 281(1789),  
920 20140846. <https://doi.org/10.1098/rspb.2014.0846>
- 921 Vigo, M., Galimany, E., Poch, P., Santos-Bethencourt, R., Sala-Coromina, J., Bahamón, N., Aguzzi, J.,  
922 Navarro, J., & Company, J. B. (2024). An update on the biological parameters of the Norway lobster  
923 (*Nephrops norvegicus*) in the northwestern Mediterranean Sea. *ICES Journal of Marine Science*,  
924 fsae003. <https://doi.org/10.1093/icesjms/fsae003>
- 925 Young, T., Fuller, E. C., Provost, M. M., Coleman, K. E., St. Martin, K., McCay, B. J., & Pinsky, M. L. (2019).  
926 Adaptation strategies of coastal fishing communities as species shift poleward. *ICES Journal of Marine*  
927 *Science*, 76(1), 93-103. <https://doi.org/10.1093/icesjms/fsy140>
- 928 Zarzyczny, K. M., Rius, M., Williams, S. T., & Fenberg, P. B. (2024). The ecological and evolutionary  
929 consequences of tropicalisation. *Trends in Ecology & Evolution*, 39(3), 267-279.  
930 <https://doi.org/10.1016/j.tree.2023.10.006>
- 931